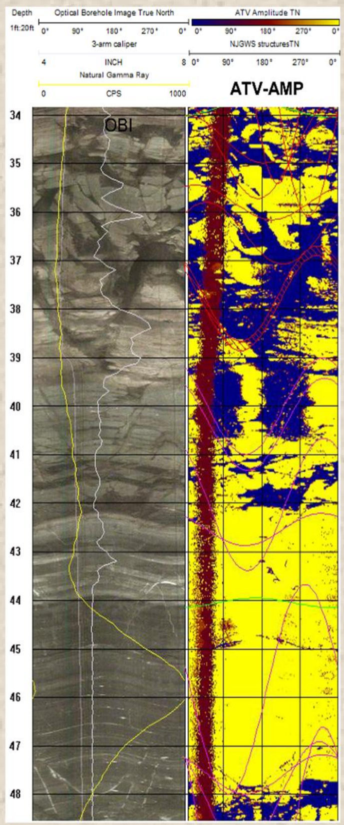

SHALLOW SUBSURFACE GEOPHYSICAL APPLICATIONS IN ENVIRONMENTAL GEOLOGY

Field Guide and Conference Proceedings

EDITED BY

Michael P. Gagliano

New Jersey Geological and Water Survey

and

Suzanne Macaoay Ferguson

PennJersey Environmental Consulting

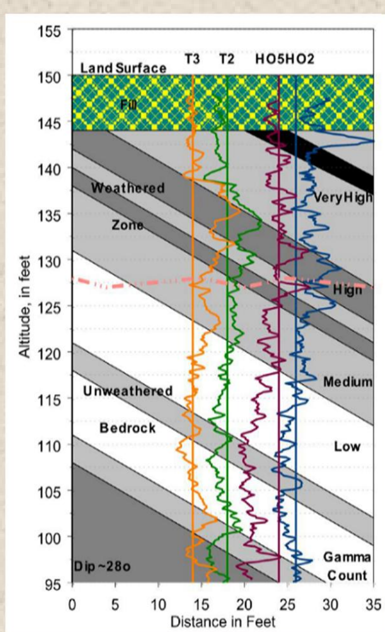

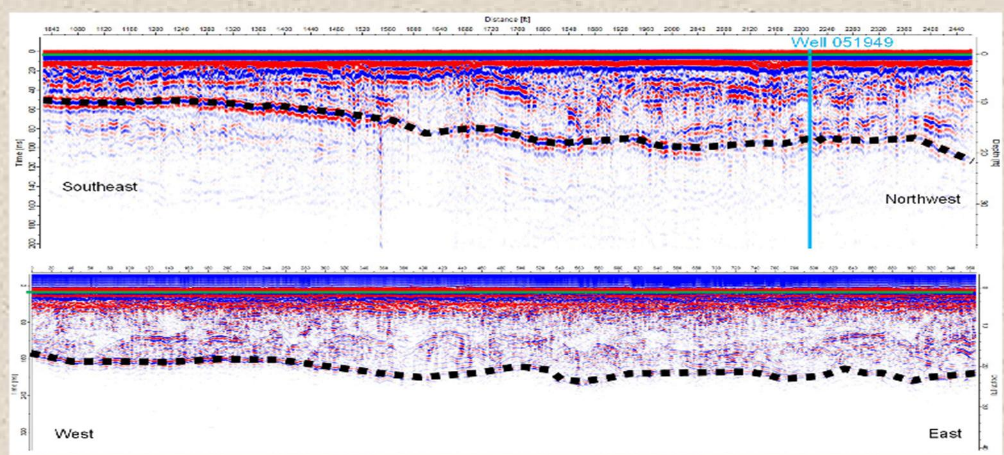

THIRTY-THIRD ANNUAL MEETING OF THE GEOLOGICAL ASSOCIATION OF NEW JERSEY

OCTOBER 14-15, 2016

THE NEW JERSEY STATE MUSEUM
TRENTON, NEW JERSEY

TABLE OF CONTENTS

Borehole Televiewer Synoptic and Hydrogeologic Framework of Adjacent RACER and NAWC Industrial Sites, West Trenton, Mercer County, New Jersey

Gregory C. Herman, Ph.D., New Jersey Geological and Water Survey (Retired)

Abstract

A detailed geological study was conducted for two adjacent industrial sites located in Trenton, New Jersey that are engaged in groundwater-pollution remedial activities. The study takes advantage of robust sets of borehole-geophysical data gathered at each site that were mostly evaluated independent of one another. The project was done because 1) these two industrial sites sit in close proximity to one another and both have a plethora of shallow subsurface information in the form of geophysical logs and cores collected over the past decade during efforts to characterize the conceptual groundwater flow models at each site, 2) because nearby Late Triassic strata are structurally inverted, which is anomalous with respect to other parts of the basin, and 3) because the Late Triassic section in this part of the Newark Basin is apparently metamorphosed to a slightly higher degree than elsewhere in the New Jersey parts of the basin. A thorough review and reinterpretation of these data sets compares and contrasts the hydrogeological framework of the fractured-bedrock aquifers at each site that happen to straddle the geological contact between sandstone-dominated clastics of the Stockton Formation and argillaceous mudstone of the superjacent Lockatong Formation. The borehole geophysical data sets include borehole televiewer (BTV) logs of both optical and acoustic types that provide good subsurface geological control for an area having a paucity of natural outcrops. For this study, 28 monitoring and test wells having BTV, natural gamma ray, and caliper (borehole diameter) logs were compiled, interpreted and structurally analyzed to determine the primary (stratigraphic) and secondary (structural) elements constituting the respective aquifer systems. The results show that stark contrasts occur between bedrock underlying each site that is reflected not only in the comparative stratigraphy but also in the structural responses to the multiple tectonic events having affected the Trenton area. This translates into having very different conceptual hydrogeological frameworks at each site. The Stockton Formation beneath the GM-RACER site displays more geological variability and is much more deeply weathered than the Lockatong Formation beneath the NAWC site. Although the average orientation of beds in both formations is similar, beds in the Stockton Formation show much greater dispersion that reflects its sedimentological origin as distributary channels in a fluvial system whereas the lacustrine beds of the Lockatong Formation are much more consistent in orientation and fracture style. The coarser, sandy nature of the Stockton Formation promotes deep bedrock weathering (~> 30m) because secondary authigenic minerals that otherwise fill tectonic fractures are commonly dissolved and removed. In contrast, the Lockatong Formation weathers to shallow depths (~<15 m) and probably behaves as a leaky-multi-unit aquifer system with a much higher degree of aquifer anisotropy.

Introduction

The results of a detailed hydrogeological study conducted during the past year in the Trenton, New Jersey area by the NJ Geological & Water Survey is summarized below using detailed subsurface geophysical logs obtained at two adjacent industrial sites having volatile-organic compound (VOC) pollution in groundwater. The site is located along the southeast edge of the central part of the Newark basin (Figures 1 to 3) The hydrogeological framework of these two sites is depicted in map and profile based on dozens of borehole televiewer (BTV) records and continuous cores obtained at the former General Motors manufacturing facility, now managed by RACER Development Corporation, and the adjacent Naval Air Warfare Center (NAWC) located immediately to the North (Figures 4 to 6). Subsurface data at each site (Table 1) were generated using multiple logging service companies on behalf a government agency and a commercial company over a two-decade time span but were previously analyzed separately with only cursory comparisons with respect to one another. The RACER site sits on Late Triassic, coarse-to-fine clastic sedimentary rocks of the Stockton Formation whereas the NAWC site is underlain by the overlying fine-grained clastic rocks and argillite of the Lockatong Formation. This study therefore straddles the stratigraphic contact between the Stockton and Lockatong Formations and provides a contrasting viewpoint of fractured-bedrock heterogeneity from both a geological and a geographic perspective. The purpose of this study is to use these robust data with modern methods of structural analysis and visualization to portray the geological complexities within the southeast-central part of the Newark Basin in the Trenton area where otherwise, outcrops are almost completely masked at land surface by deep weathering and anthropogenic landscapes. A primary goal is to compare and contrast the detailed stratigraphic and structural aspects constituting the respective hydrogeological models used to conceptualize groundwater flow in an industrial area having dissolved-phase groundwater contaminants. Data for RACER were shared with the NJGWS by Haley & Aldrich, Inc., the licensed environmental consulting firm conducting the groundwater investigation. Data for NAWC were obtained from personnel at the US Geological Survey New Jersey Water Science Center, Trenton, NJ Water Resources. The NAWC site has recently been a focus of their toxic substances hydrology program with hydrogeological research focused on mitigating groundwater pollution in complexly fractured bedrock. This work refines the geological complexities previously noted in this area using data generated during regulatory compliance work without addressing specific aspects of the latter. Stratigraphic and structural surface and subsurface details at each site are analyzed and summarized with respect to their relative positons in the Late Triassic stratigraphic sequence, and with respect to the geological heterogeneity of each formation at each site. This work therefore builds on previous hydrogeological reports while providing new insights into the local geological complexities. The data management and analysis methods employed in this study are the topic of this year’s Teacher Workshop (Chapter 1).

Geological Setting and Prior Work

This study covers the southeast-central part of the Newark Basin (Figures 1 and 2). The area is underlain by an upward succession of Late Triassic fluvial sandstone to lacustrine shale filling the basin as detailed by Olsen and others (1992). The specific location of the study straddles the formation contact between the uppermost member of the Stockton Formation (sandstone to shale) and the lowermost member of the Lockatong Formation (siltstone to argillite). The siltstone and mudrock of the Lockatong are low-grade metamorphic rock resulting from deep burial, compaction, and regional heating from early Jurassic igneous activity of the Central Atlantic Magmatic Province (CAMP; Marzolli and others, 1999).

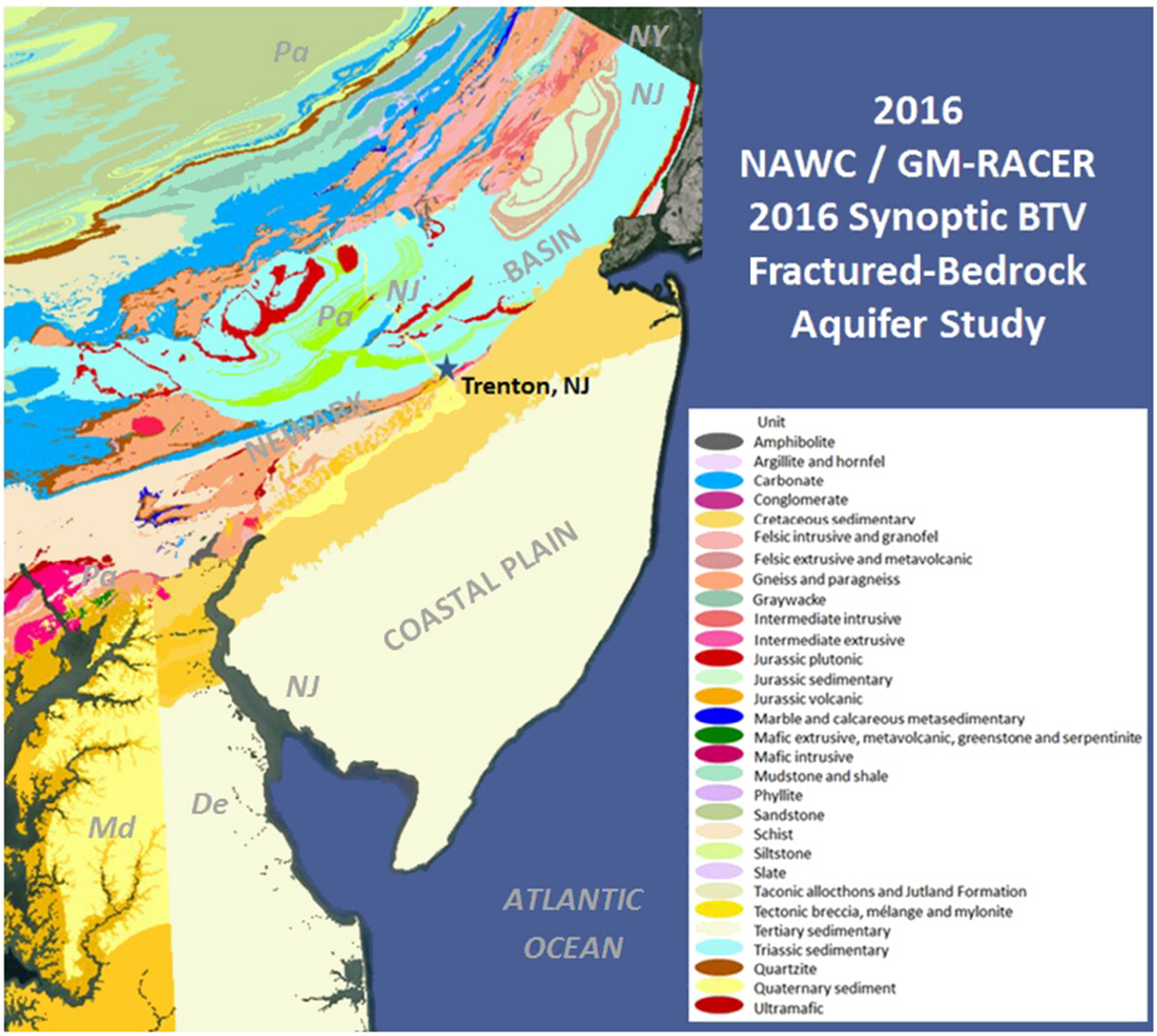

Figure 1: Regional geology map emphasizing the study location on the mid-central, southeastern border of the Newark Basin. Digital geology themes from the US Geological Survey were recompiled into a simplified regional theme for GANJ 32 (www.ganj.org/2015/Data.html).

CAMP is the large-igneous province emplaced at the onset of supercontinent breakup and the birth of the Atlantic Ocean basin (Coffin and Eldhom, 1994). The contact between these two formations is defined as the first significant gray and black shale beds in the overall course- to fine-grained stratigraphic succession leading to predominately black shale in the middle of the Lockatong Formation. The formation

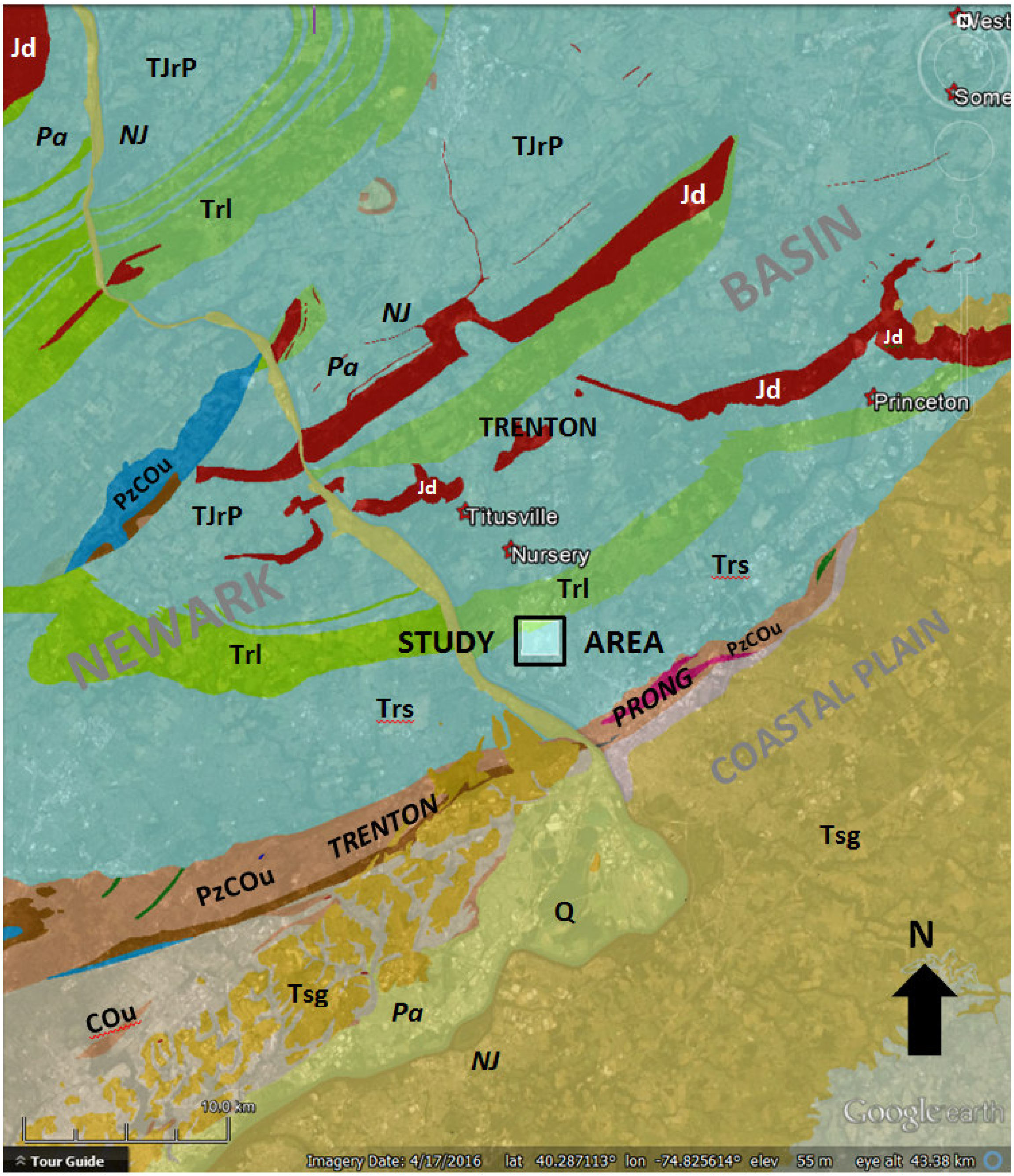

Figure 2: Geological map of the Trenton region in Google Earth showing locations of Newark Basin Coring Project cores discussed in the text (Olsen and others, 1997). Jd – Jurassic diabase, TJrp – Triassic Jurassic Passaic Formation, PzCOU – Paleozoic Cambrian-Ordovician undivided, Q Quaternary gravel, Tsg Tertiary sand and gravel, Trs – Stockton Formation, Trl – Lockatong Formation, CO- Cambrian-Ordovician undivided.

contacts are mapped differently in the State geological maps of Pennsylvania (Berg and others, 1980) and New Jersey (Drake and others; Owens and others) and shown in a regional sense by a 1:250,000 scale compilation by Lyttle and Epstein (1980). In Pennsylvania, gray and black-dominated sections are mapped as Lockatong are interdigitated with red-dominates sections of both Stockton and Brunswick Formations. Olsen and others rectified these problems but they continue to persist in digital geological coverages available from the USGS for Pennsylvania. The section of focus here is detailed in Figure 7 with nearby NBCP core and geophysical logs helping to define the penetrated section covered by these

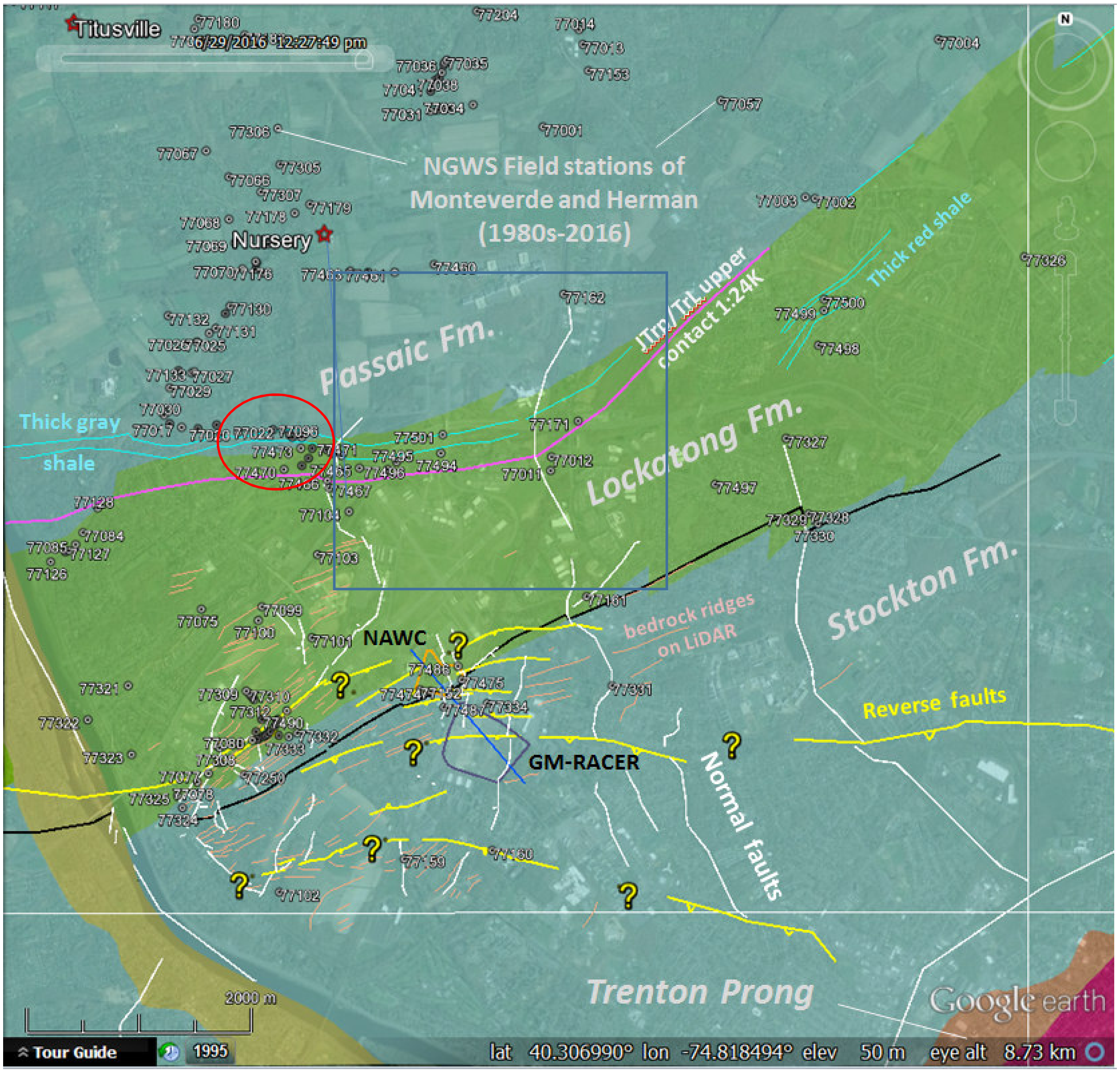

Figure 3: Geological map of the area around the NAWC/GM-RACER sites in Google Earth showing NJGWS field-station locations, bedrock ridges on LiDAR, and overlapping, inferred fault systems. The N-S trending faults are extensional faults with a major component of normal-slip and the E-W yellow faults are younger reverse faults. Red circle denotes the area of STOP 3 where structurally inverted Lockatong outcrops.

two sites. The following paragraphs are excerpts from Olsen and others (1996) that details of the stratigraphic succession in the area.

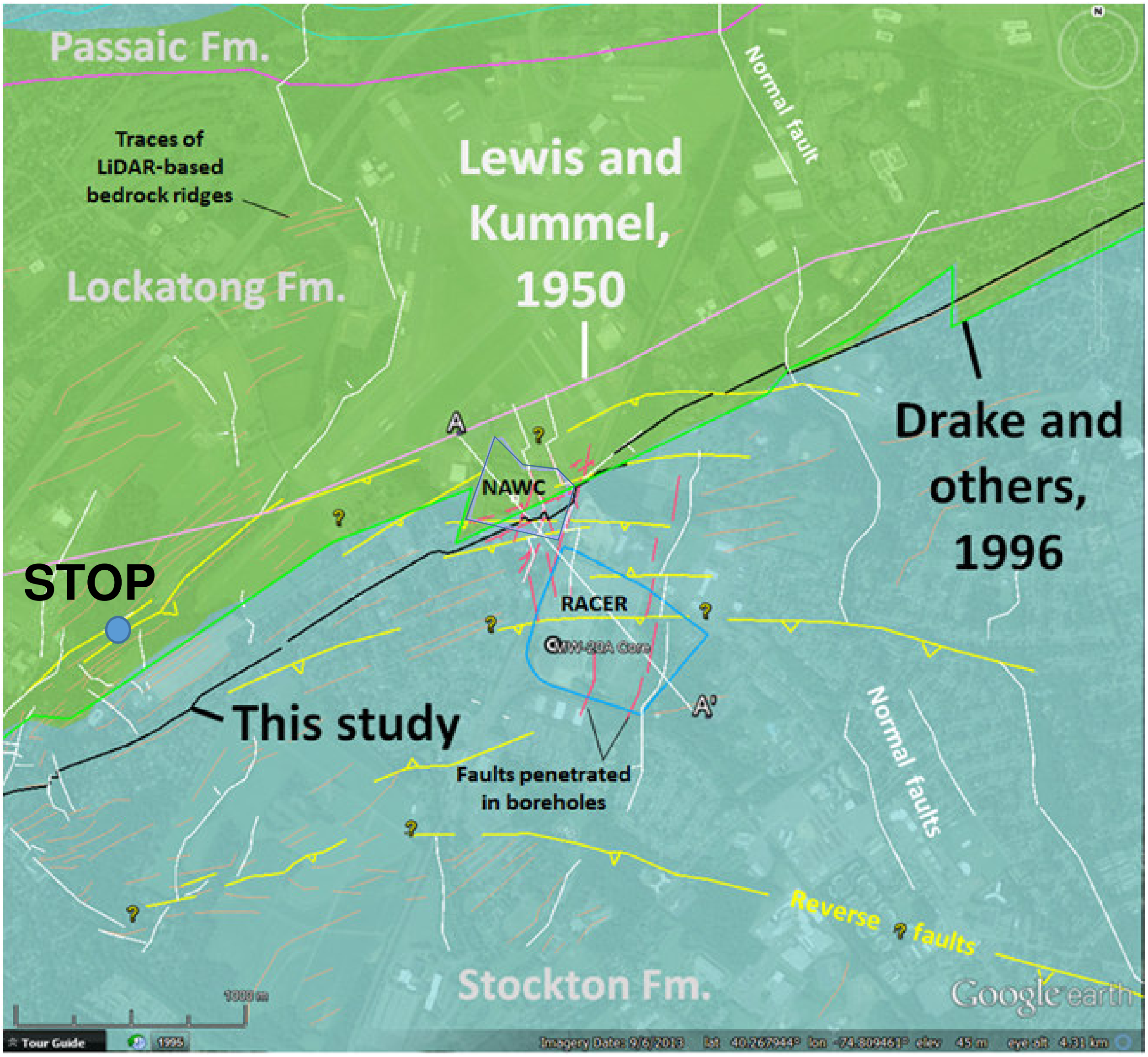

Figure 4: Geological details near the NAWC/GM-RACER sites showing different map locations of the Stockton-Lockatong formation contact. Faults penetrated by cores and outcrops in shallow excavations are colored pink, inferred (white) normal faults mostly follow streams. Stylized late-stage reverse faults are colored yellow. Note the location for STOP 3 of this year's field trip at an outcropping one.

Excerpts from: *Olsen, P.E., Kent, D., Cornet, Bruce, Witte, W. K., Schlische, R. W., 1996a. High-resolution stratigraphy of the Newark rift basin (early Mesozoic, eastern North America). Geological Society of America Bulletin 108, 40-77*

…In general, the Stockton Formation in the cores is lithologically very similar to the outcrops of the type section. The boundary between the upper Stockton and lower Lockatong formations is at the base of the lowest prominent black or gray shale sequence in the lower part of the Wilburtha Member. Comparison of the Princeton no. 1 core and the type section in outcrop suggests a correlation in which two different, but stratigraphically close, gray and black units mark the base of the Lockatong Formation, and thus the boundary between the two formations changes slightly laterally. The thickness of sedimentary cycles in the basal Lockatong Formation in its type area (as seen at Byram, New Jersey) is 177% of that in the

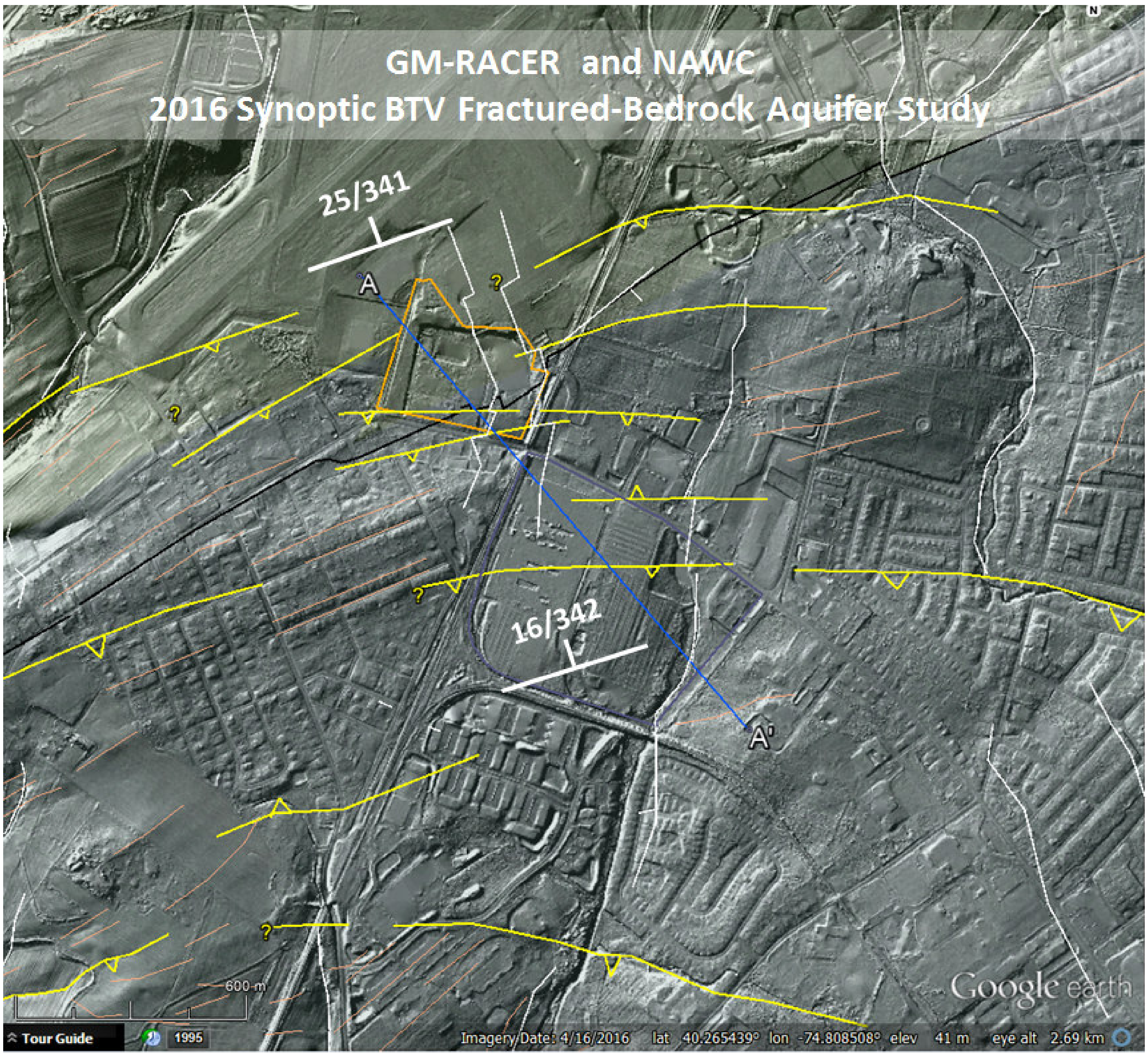

Figure 5: Tectonic elements of the area with respect to a gray, hill-shaded relief base from New Jersey LiDAR data. Note the correspondence of streams to interpreted, concealed normal faults and late-stage reverse faults (yellow) that are mostly queried because of uncertainty as to their continuity and density. The trace of cross-section traces A-A' is slightly skew with respect to average dip directions (~ 341 azimuths).

correlative portion of the Princeton no. 1 core. If the Stockton Formation in outcrop is similarly expanded relative to that in the Princeton no. 1 core, there would be a close match between the position of major sand and conglomerate-rich parts of the section. This proportional relationship between core and outcrop suggests that the members of the Stockton Formation identified by McLaughlin (1945) can be identified in the Princeton core. Overall, the Stockton Formation tends to fine upward, with the uppermost 102 m of Stockton Formation in the Princeton no. 1 core being dominated by red mudstone, as is true for the outcrop sections.

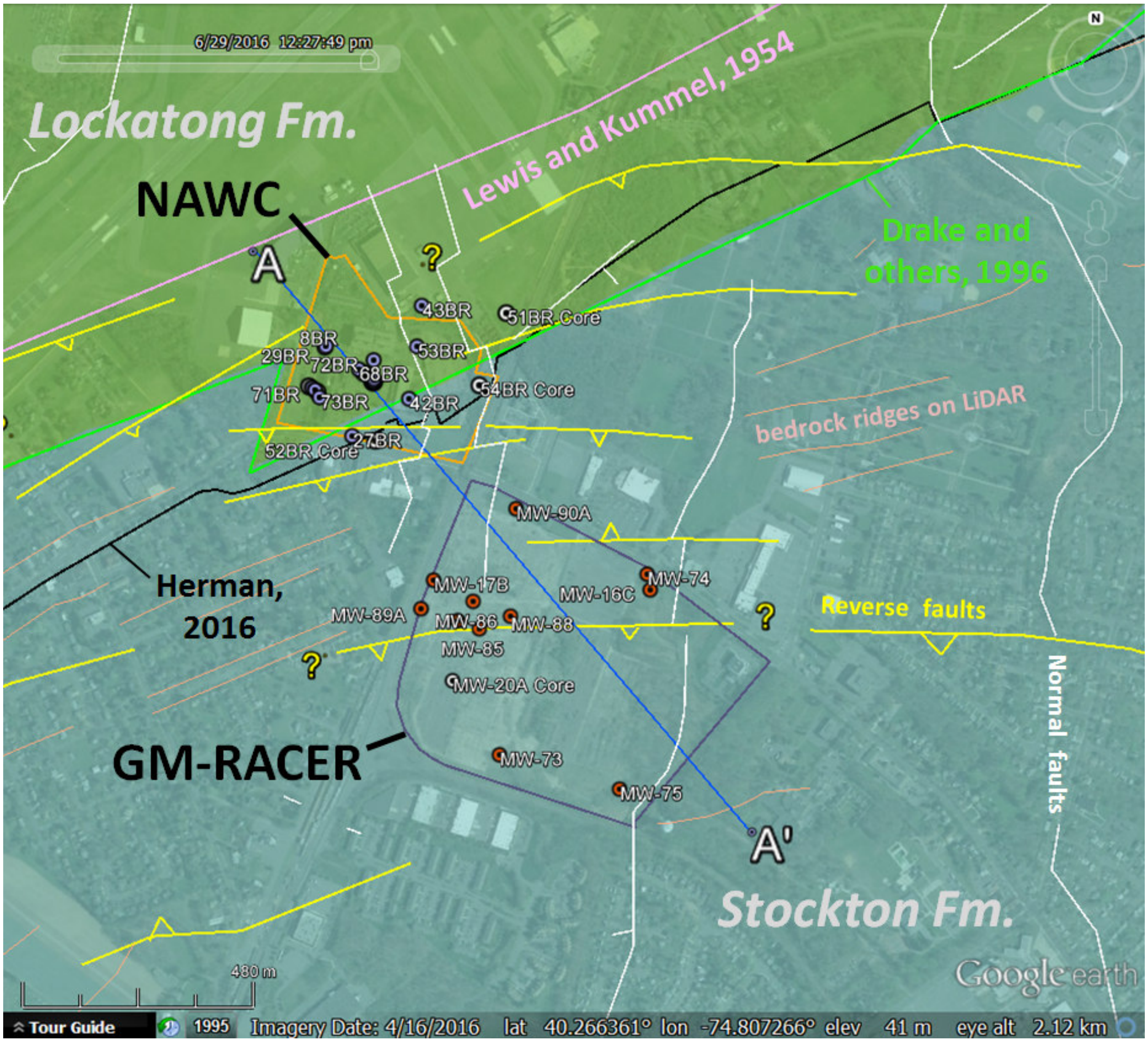

Figure 6: Bedrock geology map of the GM-RACER and NAWC sites showing the locations of wells with BTV records used in this project. Note the location of core MW-20A on the GM-RACER site.

Table 1: List of locations, depths, BTV intervals and structural attributes of wells at each site. Tilt from BTV-telemetry data indicate that most boreholes vary by less than 2° from vertical. The red-accented records highlight aspects of the radial wellfield at NAWC. The average dip and dip direction (azimuth) is highlighted for each site.

Well	LON	LAT	GE DEM (m)	BTV diam (in)	Depth (m)	OBI Top (m)	OBI Bot (m)	OBI int (m)	Avg. Tilt (deg)	Bed	Dip	DipAzm	OBI comment
GM-RACER	~270 m BTV including OBI Records												
1 MW-16C	-74.8053834	40.2650968	37.0	3.8	42.7	4.6	42.7	38.1	0.3	18/344	18	344	
2 MW-74	-74.8054573	40.2653924	38.0	3.8	41.5	5.2	41.5	36.3	0.7	17/344	17	344	
4 MW-86	-74.8097340	40.2648839	41.0	6.0	47.3	11.3	47.3	36.0	0.5	13/338	13	338	
3 MW-87	-74.8101113	40.2645228	41.0	6.0	47.3	12.5	47.3	34.8		17/342	17	342	
5 MW-88	-74.8088149	40.2646053	41.0	6.0	36.6	8.5	36.6	28.1		20/342	20	342	
6 MW-75	-74.8061350	40.2613490	35.0	3.8	34.1	6.4	34.1	27.7		19/350	19	350	
7 MW-85	-74.8095813	40.2643687	41.0	6.0	35.4	8.5	35.4	26.9		20/343	20	343	32' visibility
8 MW-90A	-74.8086797	40.2666205	41.0	3.8	32.3	12.5	32.3	19.8		13/339	13	339	
9 MW-17B	-74.8107013	40.2652822	41.0	3.8	30.8	12.2	30.8	18.6		10/340	10	340	
10 MW-89A	-74.8110100	40.2647480	41.0	3.8	19.5	12.5	27.7	15.2	0.7	8/321	8	321	21' visibility faulted?
11 MW-73	-74.8090890	40.2620030	35.0	3.8	11.6	7.0	11.6	4.6	0.8	17/360	17	360	
12 MW-20A CORE		40.2633950	41.0	3.8	242-270		Thin sections and radiometrics						200' fault Photos
							Avg. dip/dip azimuth				16	342	
NAWC	~284 m BTV including OBI Records												
1 68BR	-74.8123950	40.2691550	45.7	4.0	52.1	3.7	52.1	48.4	-	26/350	26	350	Gray
2 70BR	-74.8135320	40.2688060	45.4	4.0	32.3	1.8	32.3	30.5	1.4	24/334	24	334	Gray
3 71BR	-74.8134400	40.2687790	45.1	4.0	34.8	6.1	34.8	28.7		21/351	21	351	Gray
4 73BR	-74.8133330	40.2686430	43.6	4.0	34.5	7.6	34.5	26.9		16/354	16	354	Gray
5 84BR	-74.8121500	40.2690360	45.7	4.0	35.7	16.8	35.7	18.9		19/334	19	334	Gray
6 89BR	-74.8122140	40.2690310	45.4	9.5	35.1	16.8	35.1	18.3		18/339	18	339	Gray
7 85BR	-74.8121220	40.2690060	45.7	4.0	35.1	17.1	35.1	18.0		10/347	10	347	Gray
8 87BR	-74.8121920	40.2689590	45.7	4.0	29.9	12.5	29.9	17.4		21/343	21	343	Gray
9 88BR	-74.8122280	40.2689890	45.4	4.0	32.0	14.9	32.0	17.1		19/355	19	355	Gray
10 83BR	-74.8121760	40.2689970	45.7	4.0	33.2	17.1	33.2	16.1		21/344	21	344	Gray
11 86BR	-74.8122140	40.2690300	45.4	4.0	27.4	13.1	27.4	14.3	1.5	10/347	10	347	Gray
12 8BR	-74.8131810	40.2695800	45.7	4.0	16.5	9.8	16.5	6.7		25/327	25	327	Red w kinematics
13 42BR	-74.8111970	40.2686170	45.4	4.0	42.1	36.3	42.1	5.8		52/298	52	298	Gray and reverse sheared
14 53BR	-74.8110060	40.2695720	45.1	4.0	36.0	29.0	36.0	7.0		45/327	45	327	Gray
15 43BR	-74.8108900	40.2703150	51.5	4.0	124.7	116.8	124.7	7.9		20/332	20	332	Gray
16 29BR	-74.8132110	40.2695530	45.7	4.0	30.5	25.9	30.5	4.6		47/351	47	351	Red
17 27BR	-74.8125550	40.2679390	45.1	4.0	24.4	20.1	24.4	4.3		46/357	31	357	Red
							Avg. dip/dip azimuth				25	341	

Lockatong Formation - Kümmel (1897) named the Lockatong Formation for the mostly gray and black massive and fissile mudstones that crop out in Lockatong Creek in the western fault block. The base of the Lockatong Formation is defined as the base of the lowest prominent black or gray shale unit, and its top is defined where red beds predominate over gray. The reference section for the type area is the New Jersey Route 29 exposures along the Delaware River. In his description of the type area of the Lockatong Formation, McLaughlin (1945) divided the upper part of the formation into a series of gray and black informal units (B, A2, A1) and gave informal names to the distinctive intervening red mudstone sequences. These red gray couplets were subsequently given the informal member names of Walls Island, Tumble Falls, and Smith Corner, and the underlying four units of equal rank were named in descending order the Prahls Island, Tohickon, Skunk Hollow, and Byram members (Olsen, 1986). Below we formalize these members and provide type sections for each. The remaining lower part of the Lockatong Formation is very poorly exposed in the type area, and 5 members (Ewing Creek, Nursery, Princeton, Scudders Falls, and Wilburtha) are proposed, based on the NBCP cores. In total there are 12 members in the Lockatong Formation; the proposed new members of the Lockatong Formation, the origin of their names, their earlier informal synonyms, and locality data for the type sections are summarized in Table 2 and in data in the GSA Data Repository.[2]

[2] Geological Society of America Data Repository item 9601, P.O. Box 9140, Boulder, CO 80301.

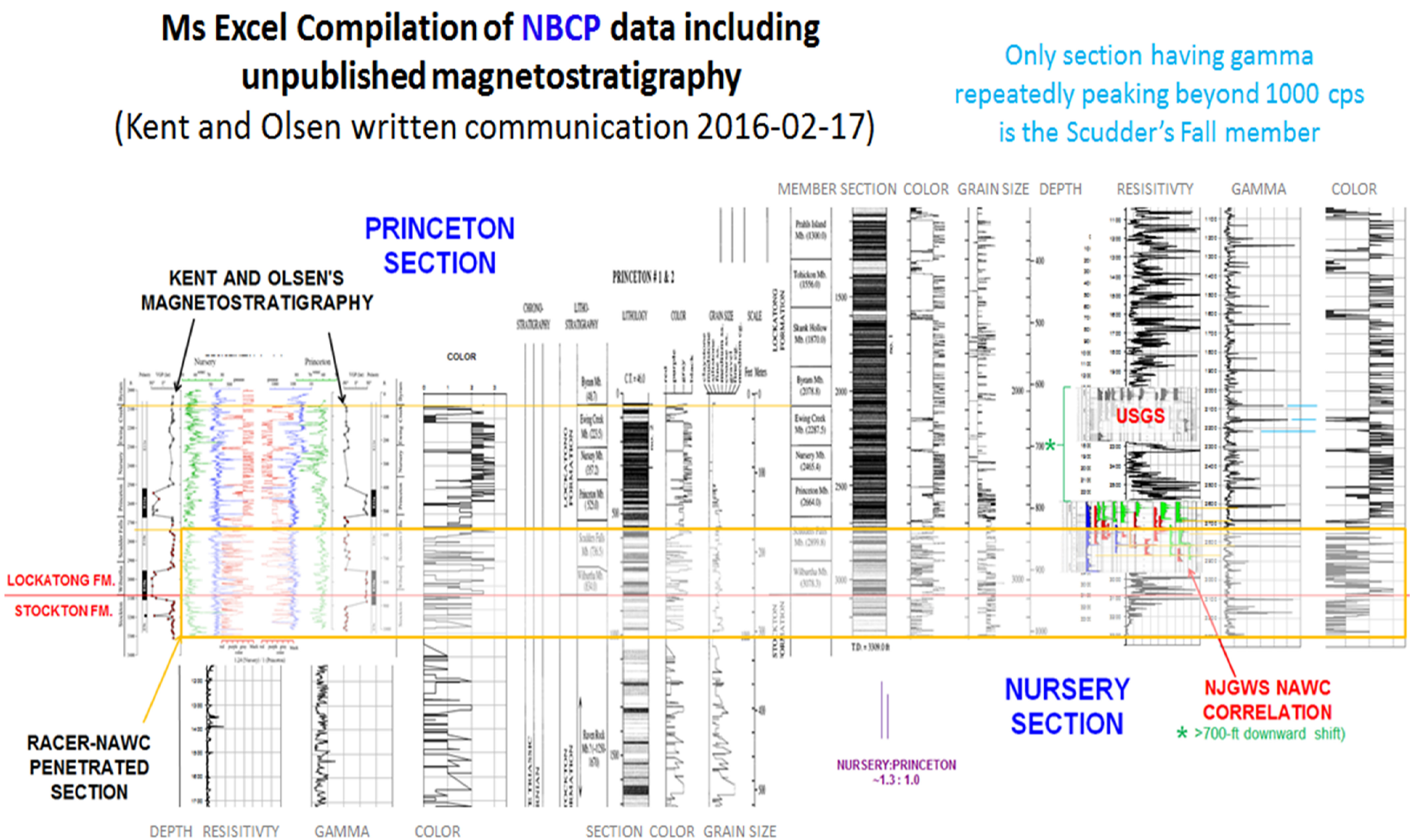

Figure 7: Stratigraphic details of the Late Triassic stratigraphic succession in the s5udy area based on the NBCP Nursey and Princeton cores that overlap the section of interest. Note that the NJGWS correlation of the penetrated section is shifted down three members relative to the former correlation by the USGS. Also note that Kent and Olsen's magnetostratigraphy is positioned in the figure relative to the Princeton core (left) and that the only section having gamma log readings repeatedly peaking over 1000 counts per second (cps) is the Scudder's Fall member near the base of the Lockatong Formation. Correlative sections of the two NBCP cores also show about 30% thickening of the section in going from the Princeton to the Nursery core.

Princeton and Nursery Core Overlap Zone - The transition from Stockton to Lockatong Formation is represented in the Princeton and Nursery cores by the Wilburtha, Scudders, Falls, and Princeton Members, and the lateral changes seen between these two cores are the largest seen in any of the NBCP core overlap zones. There is a general irregularity of the pattern of the cyclicity, so regular in the overlying section, associated with high sandstone content. However, there is still an overall correspondence in lithostratigraphy. The correlation is tested by the overall correspondence between the relative position of the E10n polarity zone, which in both cores encompasses the lowest black shales in the Lockatong Formation and corresponds to the Lockatong-Stockton formational boundary). The basal black shale of the Lockatong Formation in the Nursery No. 1 core are replaced by sandstone of the Stockton Formation in the Princeton no. 1 core. The change between these cores is best seen in the basal Princeton Member, which has several black shales in the E11n polarity zone in the Nursery no. 1 core but only one black shale in the corresponding portion of the Princeton no. 1 core. Lithological correlation between the cores markedly improves from the middle of the Princeton Member upward, and the upper boundary of polarity zone E11n occurs in both cores in excellent agreement with a matching sequence of Van Houten cycles. The details of lithology and cyclicity in the overlying Nursery and Ewing Creek members match very well between core holes.

Outcrop and near-surface data

The first New Jersey geological map (Lewis and Kummel, 1912) placed the Stockton-Lockatong contact just north of NAWC (Figures 4 and 6). The recently revised NJ geological map (Owens and others, (1998) locates the contact a little more southeastward as does the most recent, unpublished mapping by Don Monteverde for STATEMAP compilation of the Pennington, NJ 7-1/2' quadrangle, and from NJGWS research on the distribution and nature of fractured-bedrock aquifers (Herman, 1997; Herman and others, 2010). The 1998 state map also maps this contact as offset in multiple places by a system of poorly constrained, steeply dipping, normal faults that branch and splay northward from the Trenton area. These faults are left off maps shown here but their residual traces are seen where the formation contact is sharply offset along a ~N10E trend (Figures 4 and 6). Local geological details were also provided by Lacombe (2000), Lacombe and Burton (2010), and Goode and others (2014) that include a significant reverse fault along the mapped contact between the Stockton and Lockatong that contracts the section and locally omits some of the lowest members of the Lockatong section near land surface. This work shows the fault striking SW-NE and cutting the SE corner of the NAWC site (Figures 3 to 6). This USGS work also produced many unpublished photographic glimpses of the local tectonic style where small reverse faults were uncovered in excavation and rock core (Figures 8 to 10).

One particularly interesting core retrieved by Haley-Aldrich at GM-RACER has a section of massive fault breccia (Figure 9) that was generously shipped to the NJGWS for slabbing and thin sectioning (Figures 9 and 10). This autoclastic breccia in the Stockton Formation is cemented with calcite and shows significant tectonic compaction from intense mechanical twinning of the spar cement (Figure 9A). This breccia was

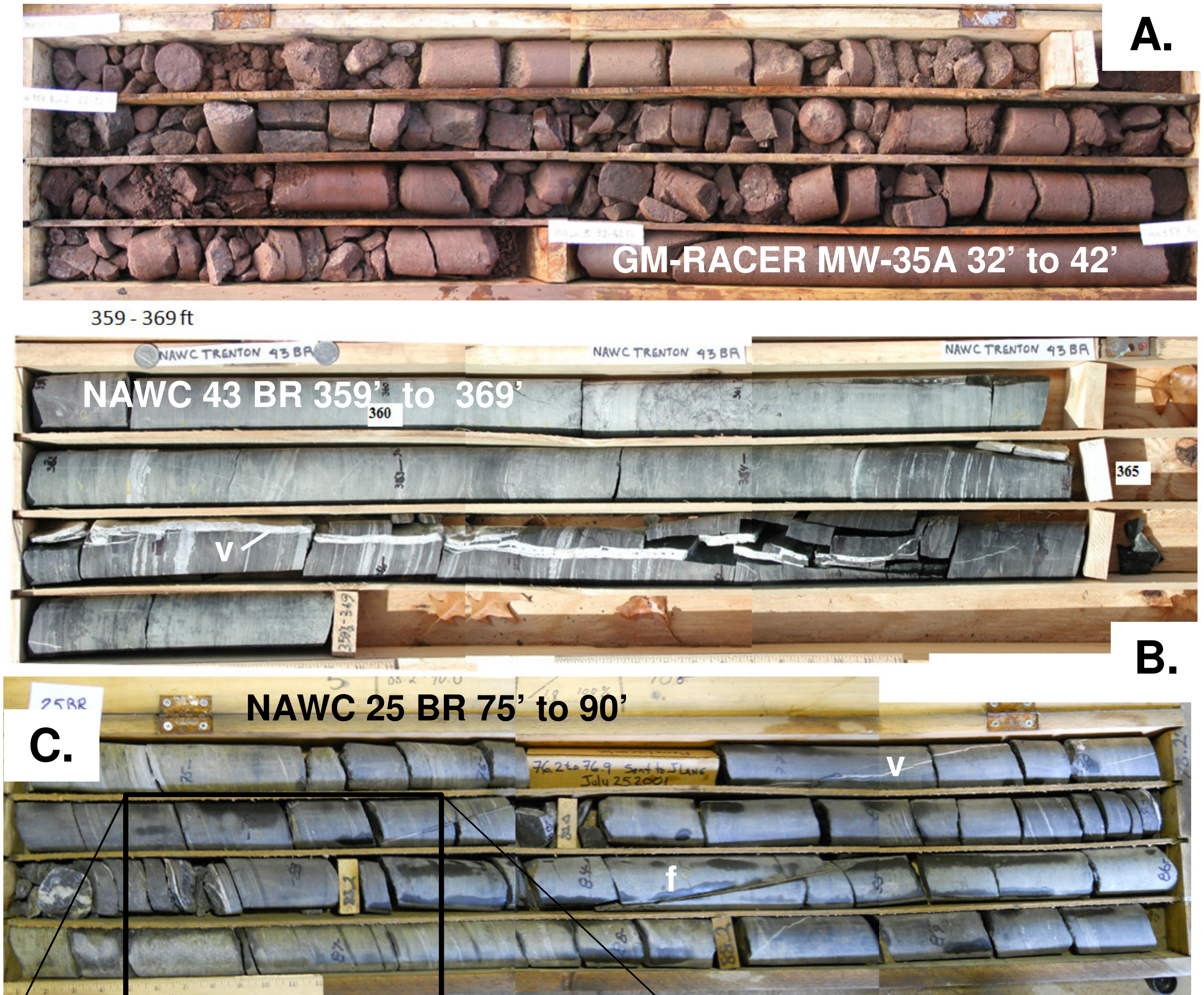

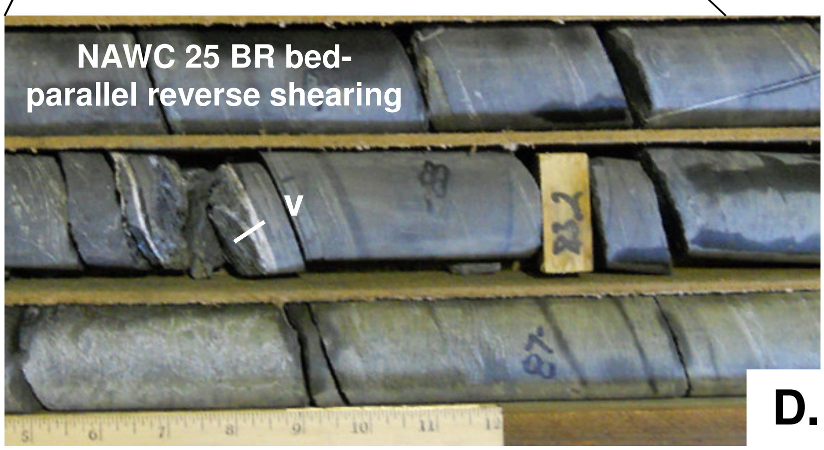

Figure 8: Representative core from GM-RACER (A.) and NAWC (B.-D.) showing lithologic contrast between the Stockton (red) and Lockatong (gray) beds. Secondary structures include steeply dipping extension fractures (f) that are commonly cemented with calcite in veins (V), and bed-parallel reverse shearing, drag folding and calcite veining (C. and D.).
Photographs by Pierre Lacombe

probably consolidated after extensional faulting of tensile origin and then overprinted by a compressive tectonic event that horizontally contracted but thickened the section with reverse shear faulting as portrayed here. Lomando and Engelder (1984) found similar compaction in rocks of the northern part of the Newark basin that aligns with other calcite-strain gauge data for bedrock of the Paleozoic foreland of Pennsylvania and New York (Engelder, 1979; Herman, 2015). We will visit overturned panels of

Lockatong strata dipping ~80^o SE that are mapped nearby in Villa Victoria Brook (Figure 3) at STOP 3 of this year's field excursion. These steeply dipping beds also likely arose from this compressional event and are the only Early Mesozoic structurally inverted strata found so far in the New Jersey part of the basin (Figure 1). The extensional and compressional structures seen in core and excavations are also seen in the BTV records.

Geological analysis of borehole televiewer (BTV), caliper and gamma logs

This project had access to a wide variety of geophysical logs collected at both sites, but mostly uses BTV records with natural-gamma-ray and caliper (borehole diameter) logs (Figures 11 and 12). Gamma logging has proven useful for correlating strata between wells in the basin using dark gray to black, organic-rich shale marker beds having noticeably elevated natural gamma ray emissions (Figure 7). Caliper logs are also critical for structural analysis and are used to derive accurate orientation measurements of geological planes in BTV records that are dependent on borehole diameter (Figure 13). BTV records include both optical (OBI – optical borehole image) and acoustic (ATV) types (Figures 10-, with the OBI being digital photographic image and the ATV including records of both acoustic-signal amplitude (AMP) and travel time (TT) responses (Figure 11) . The BTV records shown here are shown as flattened, 'unrolled' images of the borehole walls that intersect primary (stratigraphic bedding or layering) and secondary fractures and fault planes penetrated by the borehole (Figure 12). The records are interpreted in this flattened layout using WellCAD structural-analysis software module and the set of geologic and hydraulic parameters outlined in Figure 12. Sedimentological bedding and any secondary planar features such as structural discontinuities are traced and thereby measured using the amplitude and trough of each sinusoidal traced feature to determine the dip and dip direction (dip azimuth) of each plane. The mathematical details of this process are beyond the scope of this paper, but basically, gently dipping planes have low-amplitude traces that increase with increasing dip (Figure 12A).

In order to estimate the total penetrated section at each site (Figures 14 to 16) a set of logs were charted and analyzed for each well (examples given in Figures 11 and 12) and then visually compared to one another in geospatial arrangement after projection into a profile trace (Figure 15B). This process was used to assess subsurface stratigraphic continuity and the geological nature of the various fractures, shear planes, and fault zones that otherwise disrupt the section. As seen in Figures 11 through 16, the red and white beds of the Stockton Formation contrast vividly with the gray-and-black beds of the Lockatong although the boundary between these Formations is gradational and shows lateral sedimentological variation in the NBCP cores (Figure 7). The GM-RACER section covered by BTV records is estimated to span a thickness of about 60 meters whereas the NAWC section has about 130 meters coverage from gamma-log coverage and about 100 meters from BTV (Figure 17).

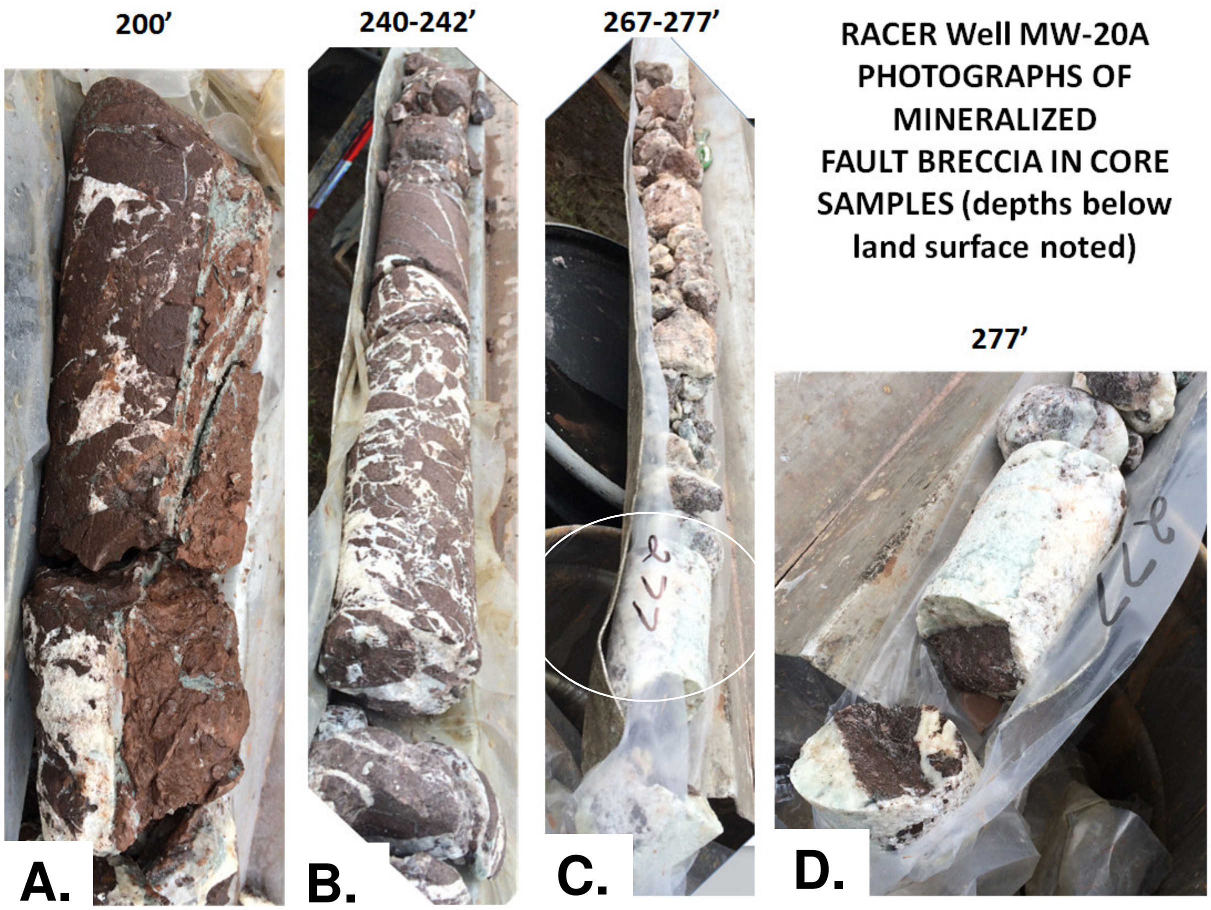

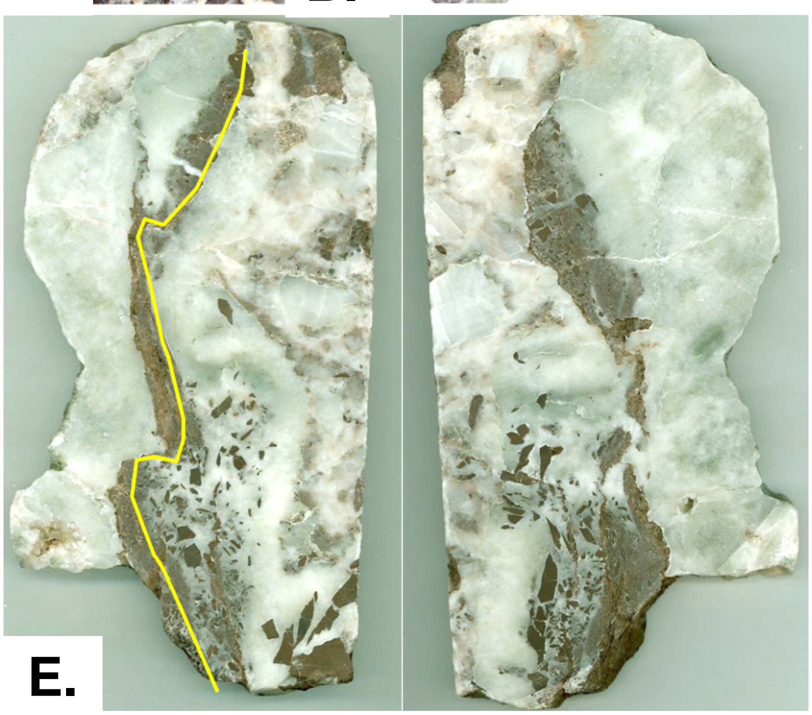

Figure 9: Photographs of 4-inch core sections retrieved by Haley-Aldrich for core MW-20A (Figure and Table 1). The respective depths of each section are noted for A-D. E is the sample from 277' (D) that was slabbed and cut for thin sections (Figure 10A).
Top photographs by Dimitri Quafsi.

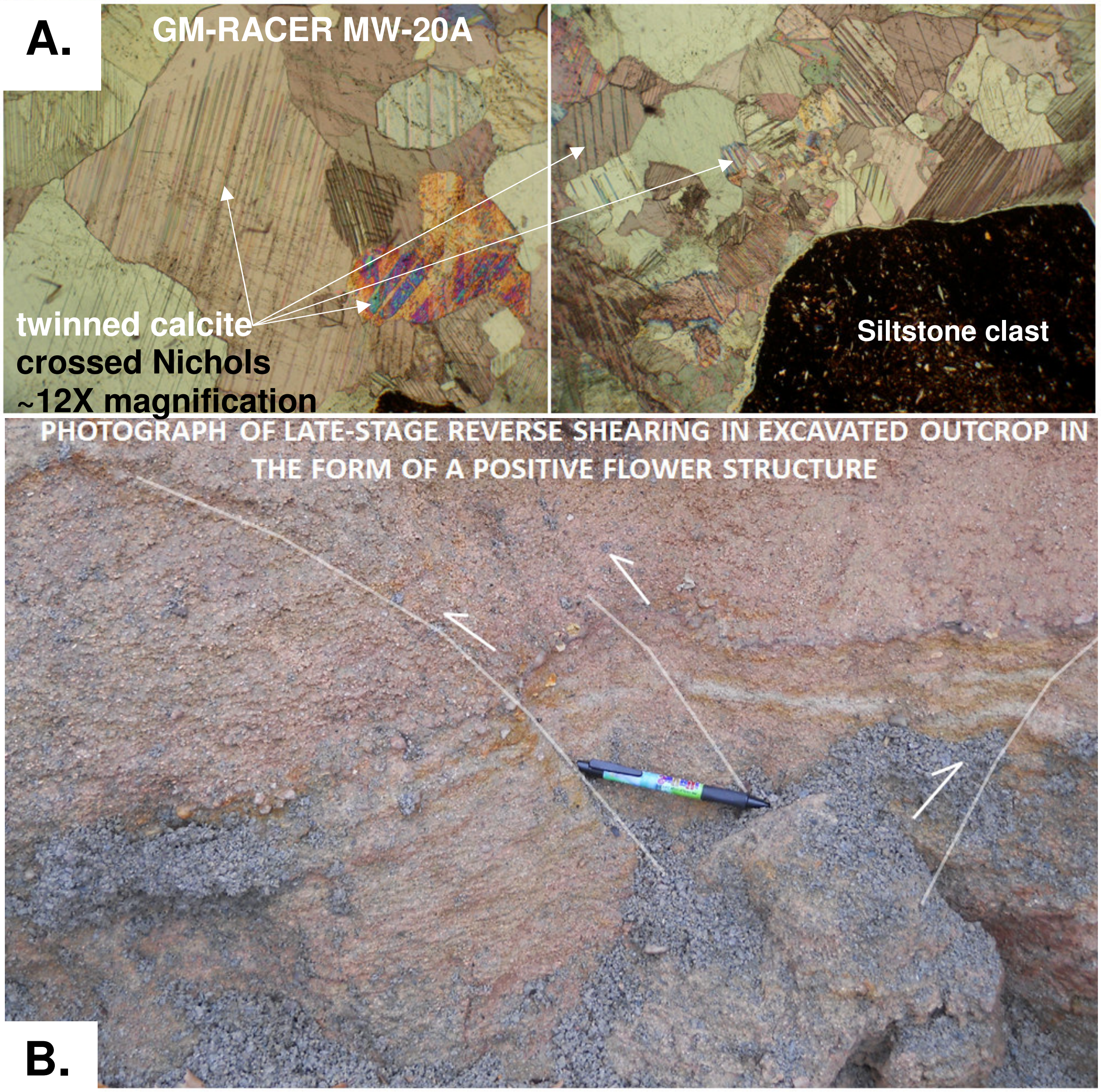

Photograph from Gold's Run 2011-11-28 by Pierre Lacombe, US Geological Survey

Figure 10: Photographs of tectonic faults in GM-RACER core **(A)** and a nearby excavation. **A.** Photomicrographs of thin sections from the slabbed core of autoclastic breccia (Figure 9E) that is calcite cemented and later tectonically compacted as seen in the extreme calcite twinning. Photo **B.** is that rare excavation that belies the structural style in the area by revealing a positive flower structure with reverse dip slip offsetting layering in Stockton Formation bedrock residuum.

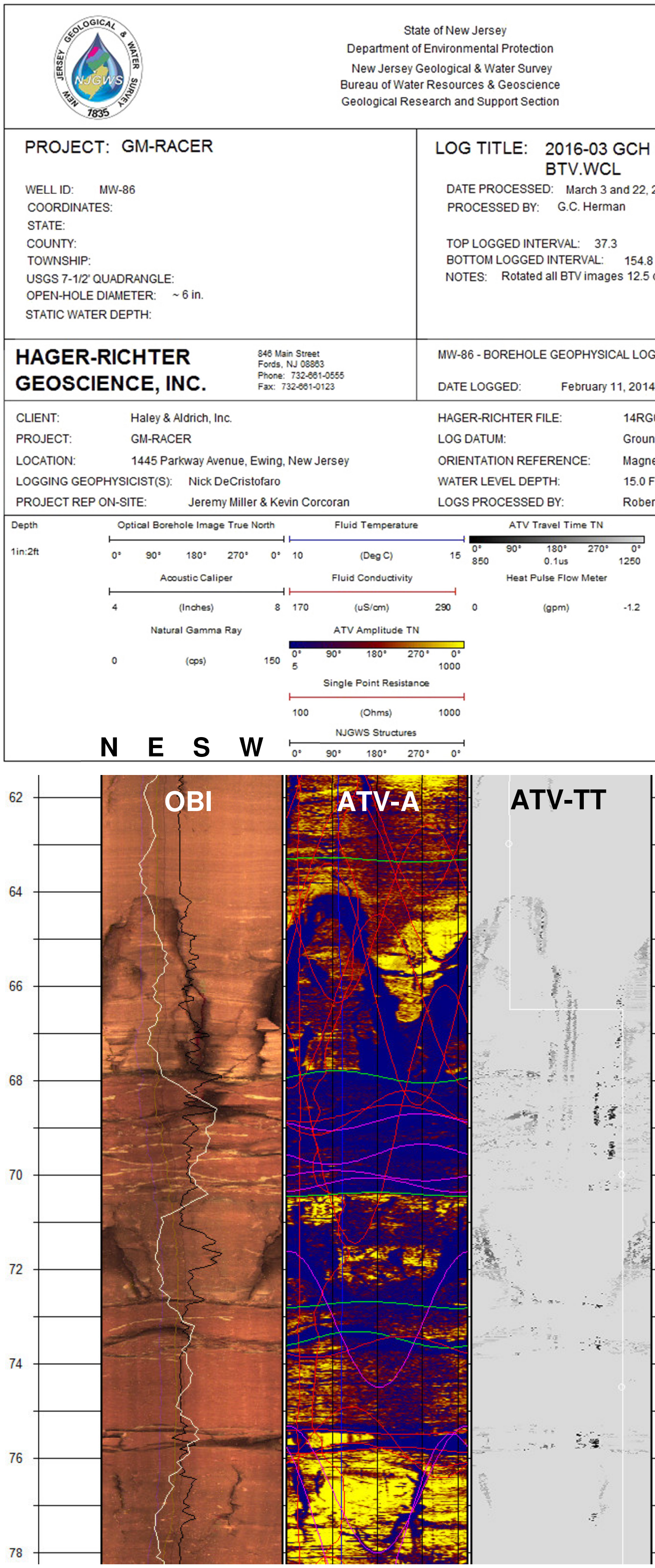

Figure 11: Example BTV logs for GM-RACER well MW-86 including the NJGWS structural interpretation overlain on the ATV-Amplitude log (middle). The OBI log is overlain with acoustic caliper (borehole width) as black-line trace and a natural gamma ray log (white line trace). Interpreted structures include bedding (green line trace and Type 1 of Figure 10), fractures (red line traces and Type 6), and veins (or mineralized fractures – purple line traces and Type 7).

The beds at NAWC dip at a slightly steeper angle (~ 25°) than those at GM-RACER (~16°, Table 1) so even though the site spans are similar, NAWC has more stratigraphic coverage. The stratigraphic details at NAWC match the NBCP records closely when correlated with the upper part of the Wilburtha and lower part of the Scudder's Fall members of the Lockatong Formation (Figure 7). In particular, the multiple gamma-log responses exceeding 1000 counts per second (cps) for this interval are not only among the highest responses seen in the Lockatong Formation, but the entire > 6km-thick section of Early Mesozoic strata in the NJ part of the basin (Olsen and others, 1997; Herman, 2010).

A detailed structural analysis was completed for each well record using both OBI and ATV imagery (Figures 11 and 12). Feature planes were categorized using the geological criteria listed in Figure 13B and Table 2. Upon completion, feature orientations and annotations were exported from WellCAD into ASCII text files that were used for data sorting and structural analyses. Bed, fracture, shear plane, and fault orientations were analyzed first for individual wells (Figures 17 and 18) and then grouped for each site to compare structures in contrasting lithologies (Figures 19 and 20). Circular histogram and stereonet structural analyses used GEOrient ver. 9.5 software. Care was taken to

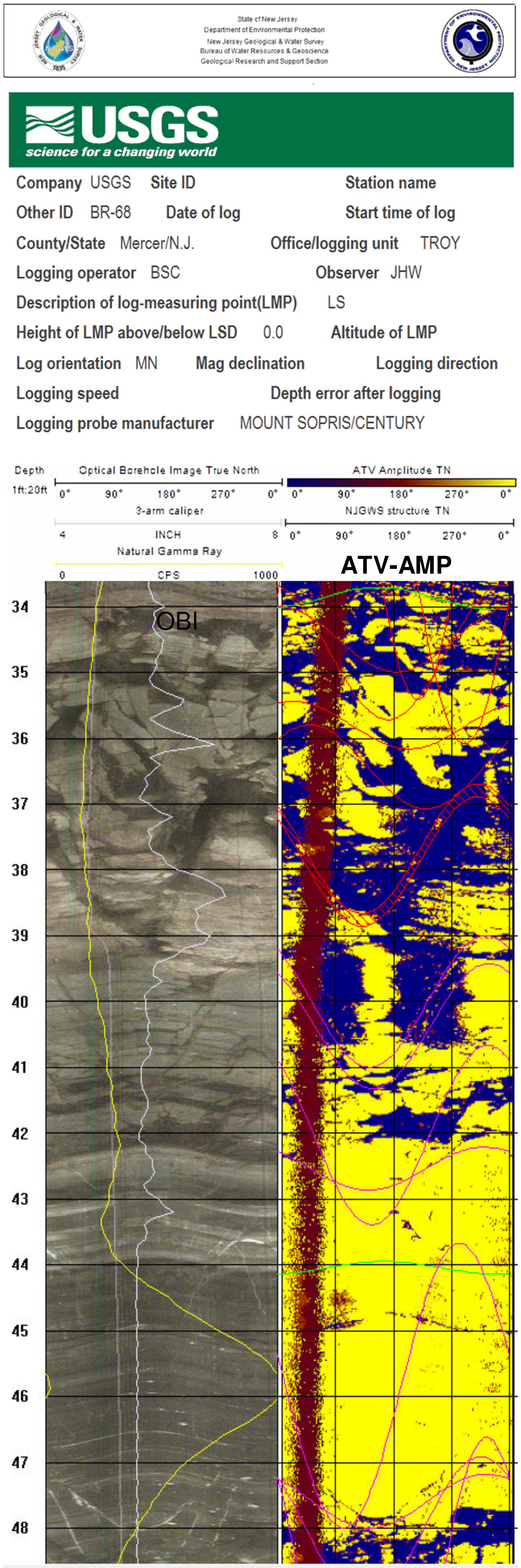

Figure 12: Interpreted section of NAWC well BR-68. The NAWC records acquired from the USGS include an optical borehole image (left) that is overlain with line traces of the borehole caliper (borehole thickness - white line) and natural gamma ray (yellow) logs. This OBI record shows an upward succession of dark- to light-gray sequence capped by a pink layer before returning to gray. This section also includes the gray bed with a gamma-response exceeding 1000 cps that facilitates stratigraphic correlation (Figures 7 and. 15A). The middle gamma-log trace in the Scudder's Falls Member is the most pronounced of three high-gamma kicks in this section (Figure 7).

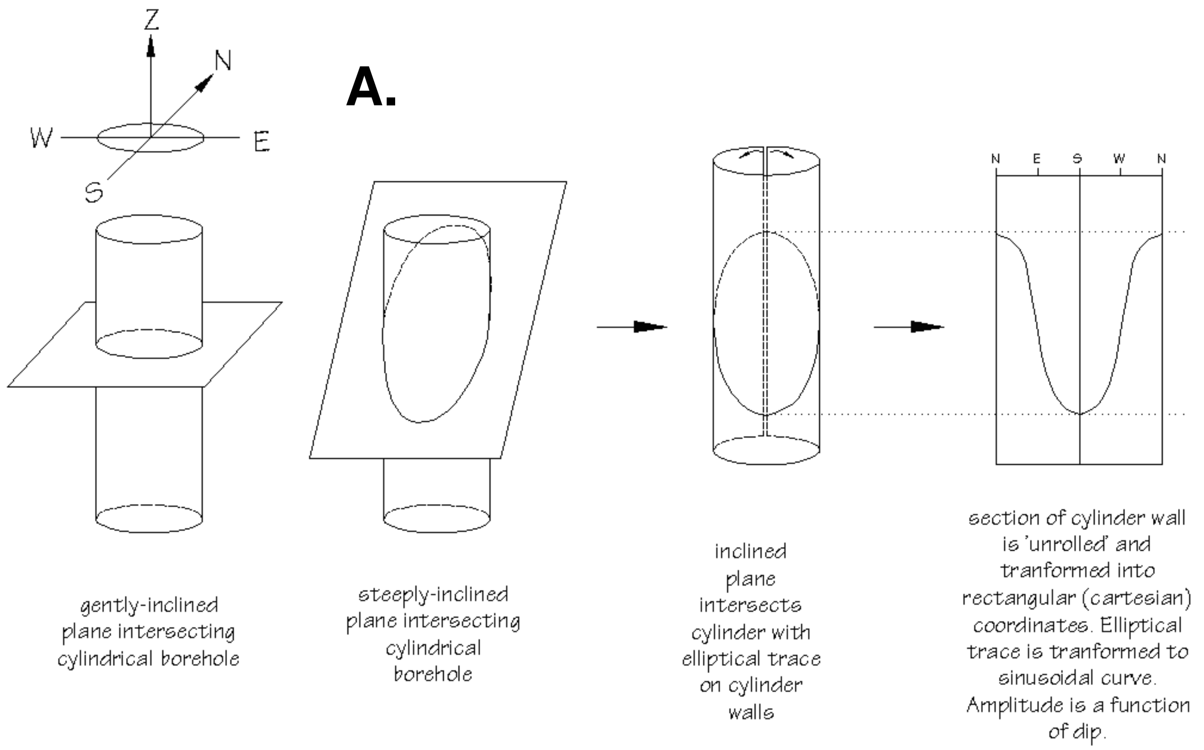

TYPE → KIND → SENSE → PERMEABLE → ALTERED

TYPE →
- 0 - Broken Zone / Undifferentiated
- 1 - Bedding
- 2 - Metamorphic layering
- 3 - Metamorphic foliation
- 4 - Igneous layering
- 5 - Igneous foliation
- 6 - Fracture
- 7 - Vein
- 8 - Cleavage
- 10 - Shear plane
- 9 - Fault zone

KIND →
- 1 - Fracture
- 2 - Interval
- 3 - Shear
- 4 - Extension
- 5 - Sealed
- 6 - Open
- 7 - Zone

SENSE →
- 1 - Reverse
- 2 - Normal
- 3 - Oblique
- 4 - Left lateral
- 5 - Right lateral
- 6 - Crosses
- 7 - Cuts

PERMEABLE →
- 0 -
- 1 - Permeable

ALTERED
- 1 - Staining
- 2 - Alteration
- 3 - Mineralized

B.

Note: TYPE is the primary criteria. Fracture is repeated in TYPE and KIND categories so that fracturing subparallel to bedding ($\pm 5^\circ$ strike and dip) can be noted (bed, fracture) and treated separately from non-bed-parallel fractures. All secondary criteria are optional.

Figure 13: A. Schematic diagram illustrating how cylindrical BTV records are processed by 'unwrapping', flattening, and transforming borehole data. The trough of the trace (or the bottom of the 'V') gives the structure dip azimuth. Higher dips correlate with sharper Vs. **B.** The systematic ranking criteria used at the NJGWS for interpreting BTV records (ca. 2000-2016).

Table 2: Geological variables used to catalogue measured structural features for this study.

1 - bed or layer
2 - fracture (uncemented)
3 - vein (cemented)
4 - shear plane
5 - fault zone

Please note: *Structural planes coded as 1 - 5 can have secondary variables denoting additional mineralization, alteration, staining, and permeability. Shear planes and faults can also include normal or reverse secondary notation. Beds were measured along sedimentological traces in OBI records and can include a secondary fracture variable used to spatially discriminate sections having little to abundant bed-parallel fracturing.*

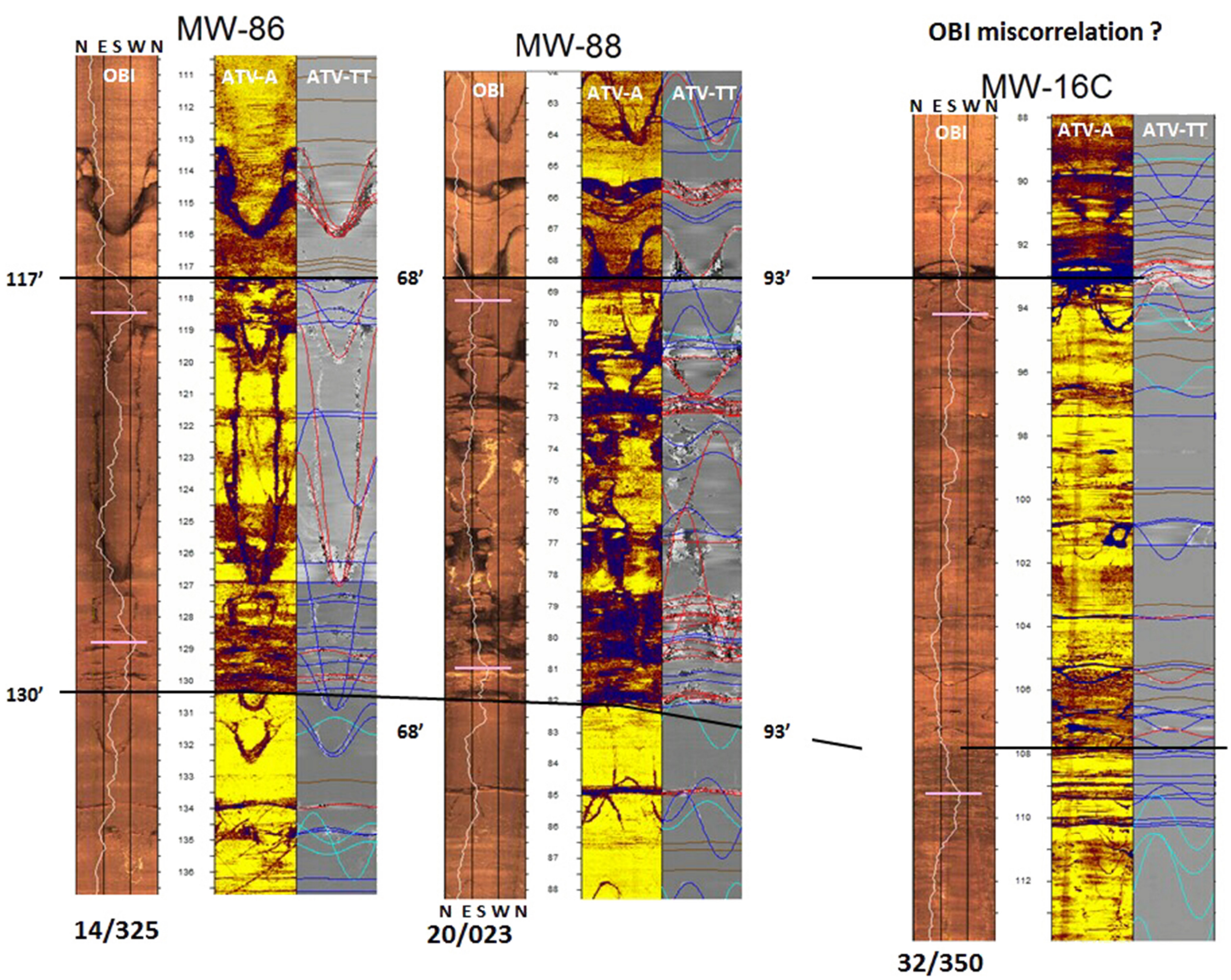

Figure 14: Example BTV sections for three wells at GM-RACER having both optical (OBI) and acoustic (ATV- Yellow Amplitude and Gray Travel Time). White gamma-log traces are overlain on the OBI records and Hager Richter's structural interpretation are overlain on ATV Travel Time (TT) logs. The left two logs show a definite stratigraphic correlation whereas the other is similar but not the same.

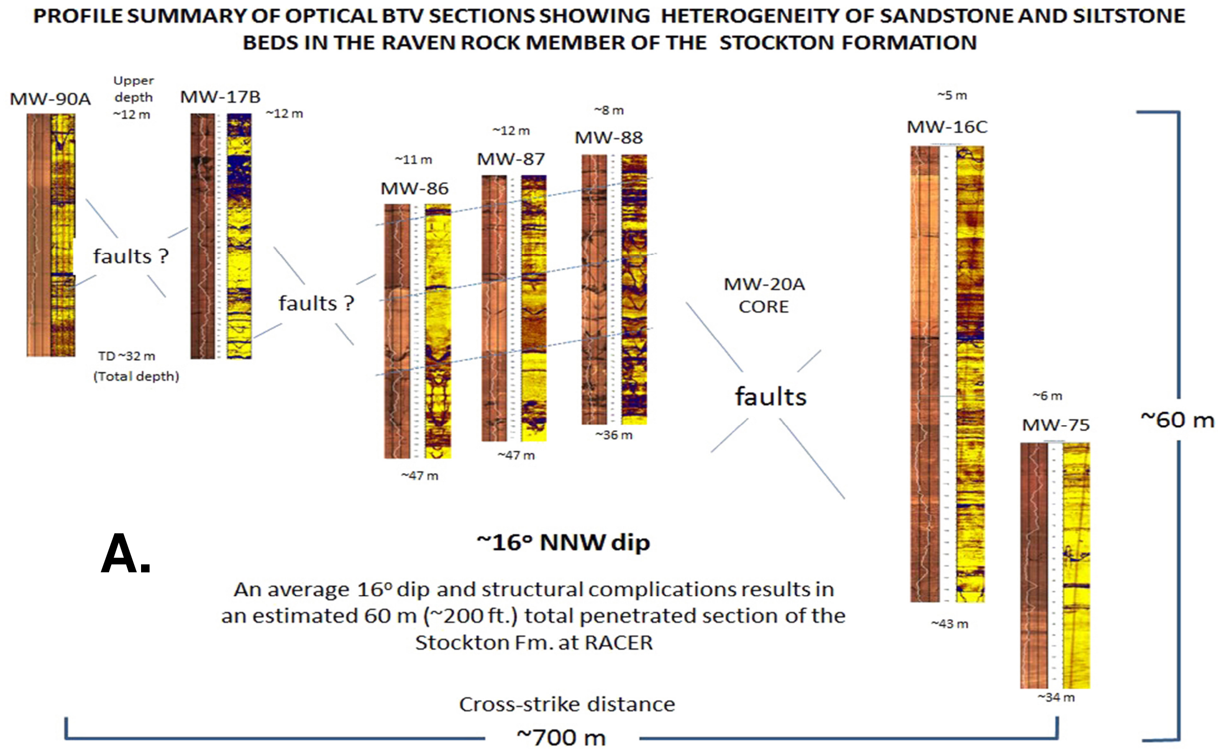

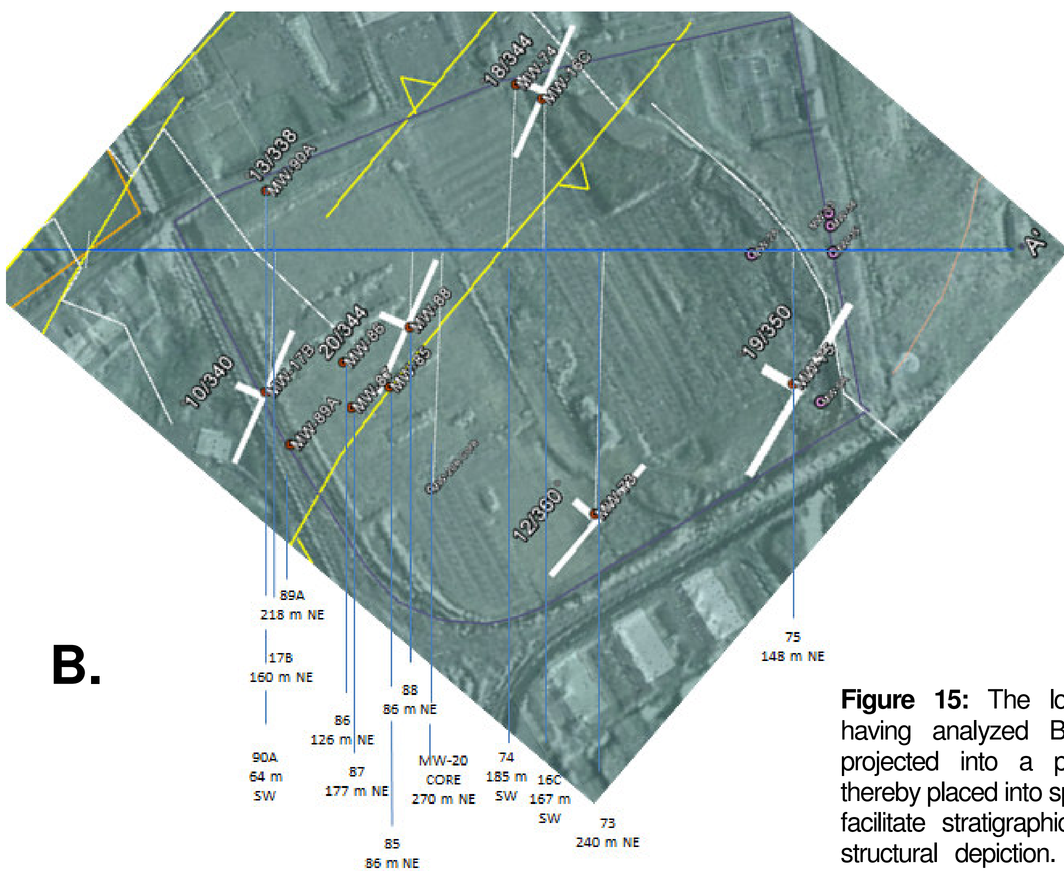

Figure 15: The locations of wells having analyzed BTV records are projected into a profile trace and thereby placed into spatial alignment to facilitate stratigraphic correlation and structural depiction. As seen in A., there are uniformly dipping panels that are structurally offset along fault zones.

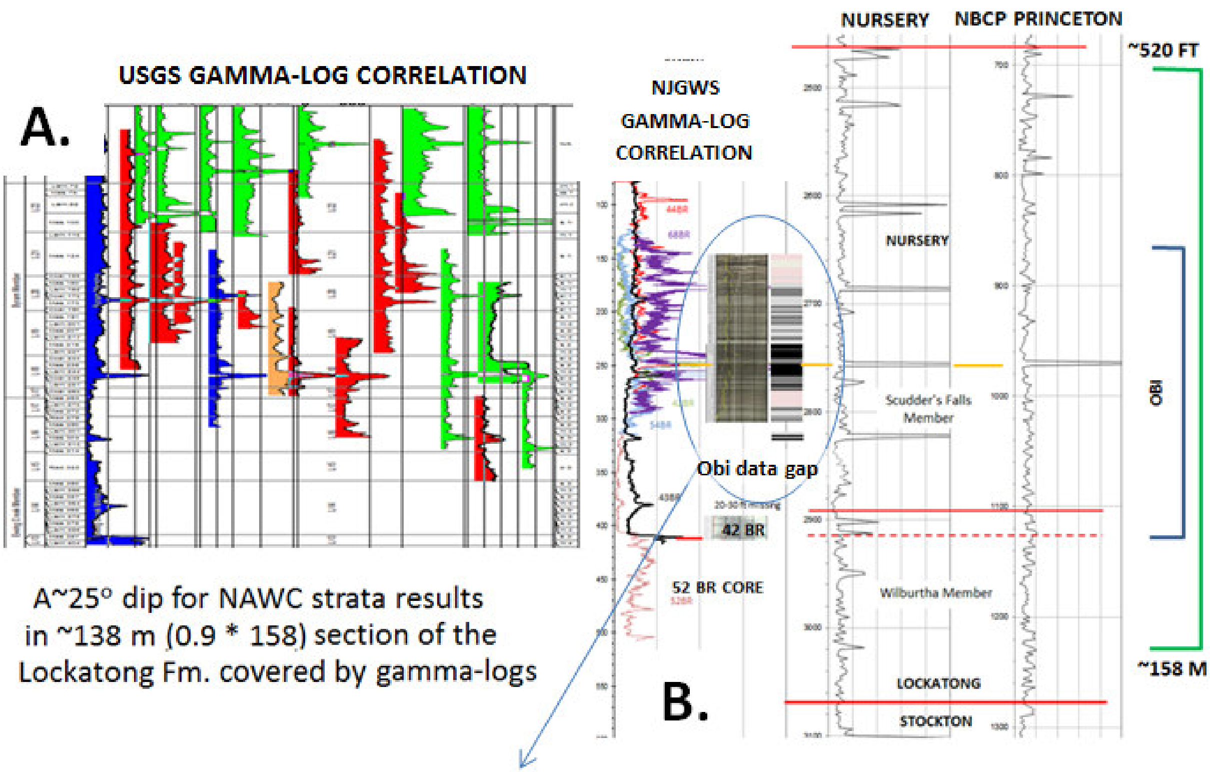

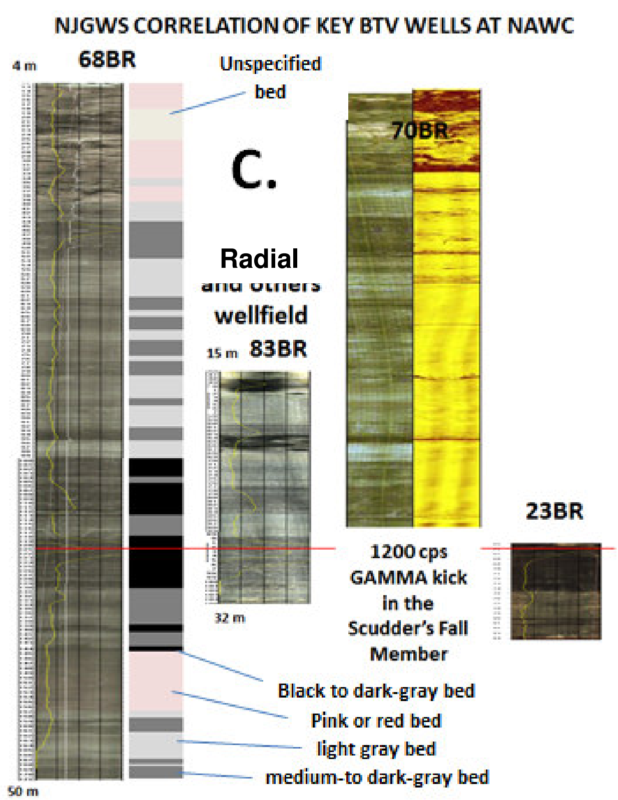

Figure 16: Detailed stratigraphic correlation for NAWC based on the USGS gamma-ray log correlation and BTV logs. **A.** The USGS gamma correlation summarizes the stratigraphic uniformity across the NAWC site. **B.** The NJGWS interpretation integrates the NBCP records with those at NAWC using a MS-Excel worksheet to combine log traces with screen-captured BTV imagery for OBI records 68 and 42 BR as detailed in **C.** Note how the positive gamma-log 'kick' in the middle of the Scudder's Fall member is the largest and most consistent in the NBCP records. There is ~160 m of gamma-log coverage of the Lockatong section at NAWC and ~50 m of BTV coverage. **C.** summarizes the NJGWS correlation of key BTV wells at NAWC and includes a schematic section noting the succession of multi-colored beds.

differentiate mineralized fractures (veins) from unhealed ones. Bed orientations are based on traces of sedimentological features rather than bed-parallel fractures that were noted separately to spatially account for sections having little or abundant bed-parallel fracturing, presumably stemming from erosional unroofing or glacial loading and unloading processes. For this project, the main classes of feature that were noted and catalogued as part of the NJGWS geophysical log library are specified in Table 2.

The NJGWS method of BTV analysis differs slightly from most commercial contractors that focus on fractures that are potentially permeable in order to cover potential pathways constituting the hydrogeological framework. Some cemented fractures are not seen in ATV records because their acoustic properties vary little from the host rock. ATV records therefore are useful for imaging structures through turbid water that can obscure optical records, but they cannot be solely relied upon to provide a thorough structural and tectonic analysis. The best approach is to use both OBI and ATV records to interpret structural features. More details about NJGWS methods of interpreting BTV records are provided in this year's teacher's workshop (Chapter 1).

Shear planes and fault zones are mapped based on visual indicators of structural discontinuity and offset of strain markers like bed forms and early fractures cut and offset by later ones (figure 21). Observed shear in BTV records was modeled using Trimble Navigation, Inc.'s SketchUp 2015 computer-aided drafting software. Borehole models were manually constructed using intersecting planes of know orientations and shear slip, manually offsetting cut structures, and then unrolling them to see how they look in the 'flattened' perspective that BTV-processing software relies upon. To date, models have only been constructed of small dip-slip shears as visual references to help resolve the nature of apparent offsets observed in BTV records (Figures 21 and 22). It is usually time and cost prohibitive to resolve kinematic solutions to a higher degree when using BTV records for groundwater evaluations, but the methods exist for subsurface mineral exploration at a price (for example see http://vektore.com/).

Cross-section analysis including structural profiling of fractures using stereonet statistics and apparent dips

The profile depiction of the hydrogeological framework (Figures 24 and 25) was built using Google Earth (GE) and Microsoft (MS) PowerPoint software. GE was used to extract a screen-captured image of the topographic profile that was pasted into PowerPoint for tracing as a freeform polyline (Figure 23). After many years of representing digital geological form in profile, I have come to rely on MS PowerPoint software for communicating this type of information as it provides a multipurpose, widely used, and multifunctional platform for graphics production that includes options for specifying object rotation angles and line length by accessing object-property dialog boxes. For example, the profile boundaries are augmented with depth and length graticules of specific length. MS PowerPoint therefore provides possesses the necessary functions to easily representative geological structures to be depicted in profile at their apparent dip angles. This is done by calculating apparent-dips for each structure and simply rotating lines into position at known locations using built-in software functions. Examples of this process are demonstrated in Chapter 1.

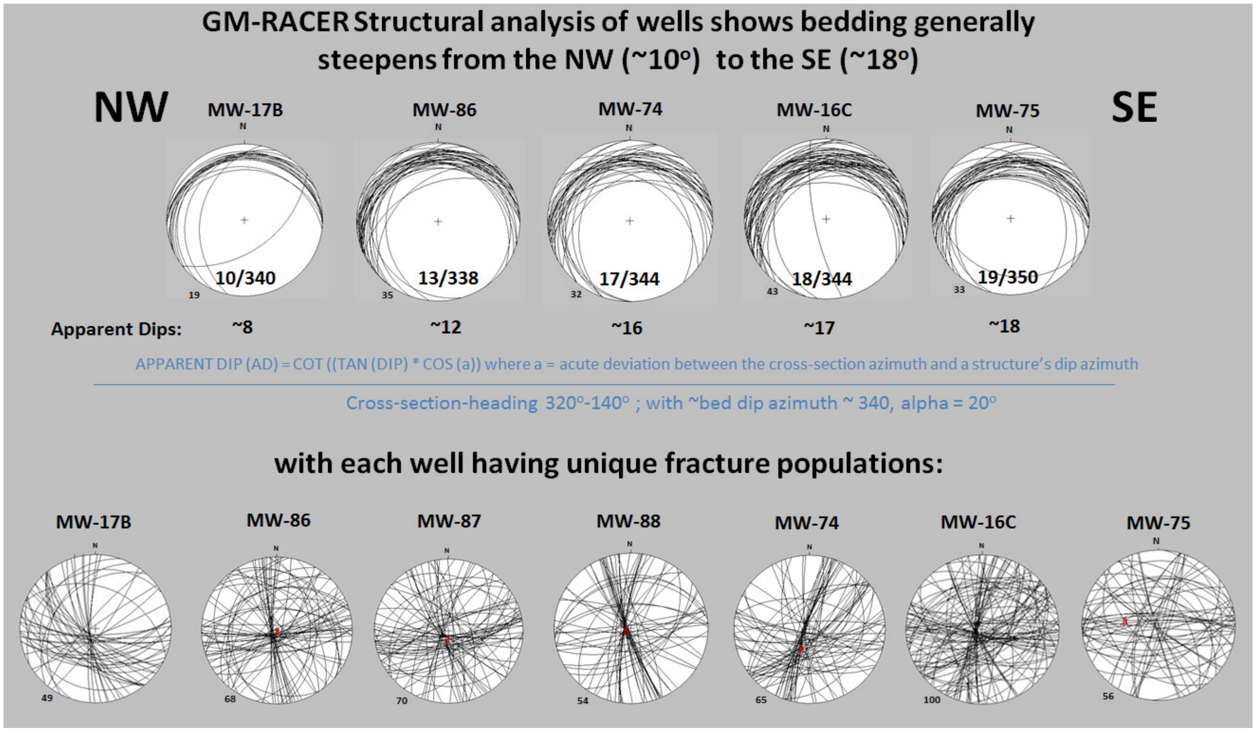

Figure 17: Stereonet structural analysis of the GM-RACER wells showing bed dip steepens across the site from NW to SE. Note that the apparent dips of bedding used in the cross section are close to true dips and each well has a unique fracture population (bottom).

BTV data were projected into cross-section A-A' as the primary control for constructing a profile interpretation of the conceptual hydrogeological framework (Figures 23 to 25). Some well records overlapped in places when projected into profile and were culled from the depiction to help preserve graphic clarity. In those instances, the most pertinent record was represented, usually predicated by having the thickest imaged section or deepest penetration. The process of constructing the profile depicted in Figures 24 and 26 involved the steps outlined below.

a) Generate the topographic profile using GE (Figure 24) and develop section boundaries from the section trace.

b) Project each well location into profile (Figure 15B) and represent their sub-vertical trace with simple lines scaled to the appropriate size depicting cased and open sections (Table 1).

c) Project mapped stratigraphic contacts and fault traces onto the surface trace along with any

d) Project primary and secondary geological structures gained from BTV analysis of each well, or group of wells, into profile using apparent-dip values of structural features determined from stereonet analysis. This requires knowing the deviation angle between the dip azimuth of each representative structure and the azimuth of the cross-section trace (Figure 23). For a simple graphic depiction of apparent versus true dip, please see www.impacttectonics.org/GEO310/Labs/3A-Apparent_Dip.pdf.

e) Stylize the section components to reflect the observed geometry of primary and secondary structures identified in the BTV structural analyses. For example, offset primary and secondary structures by younger ones as observed from kinematic analyses (Figure 21).

As seen in Figure 24, overall BTV coverage is good but a significant data gap occurs in the middle of the section between the sites where the major reverse fault is mapped by Lacombe and Burton (2010). Nevertheless, these BTV data provide geological coverage for thick sections of the upper member of the Stockton Formation and lower members of the Lockatong Formation (Figure 7). The comparative

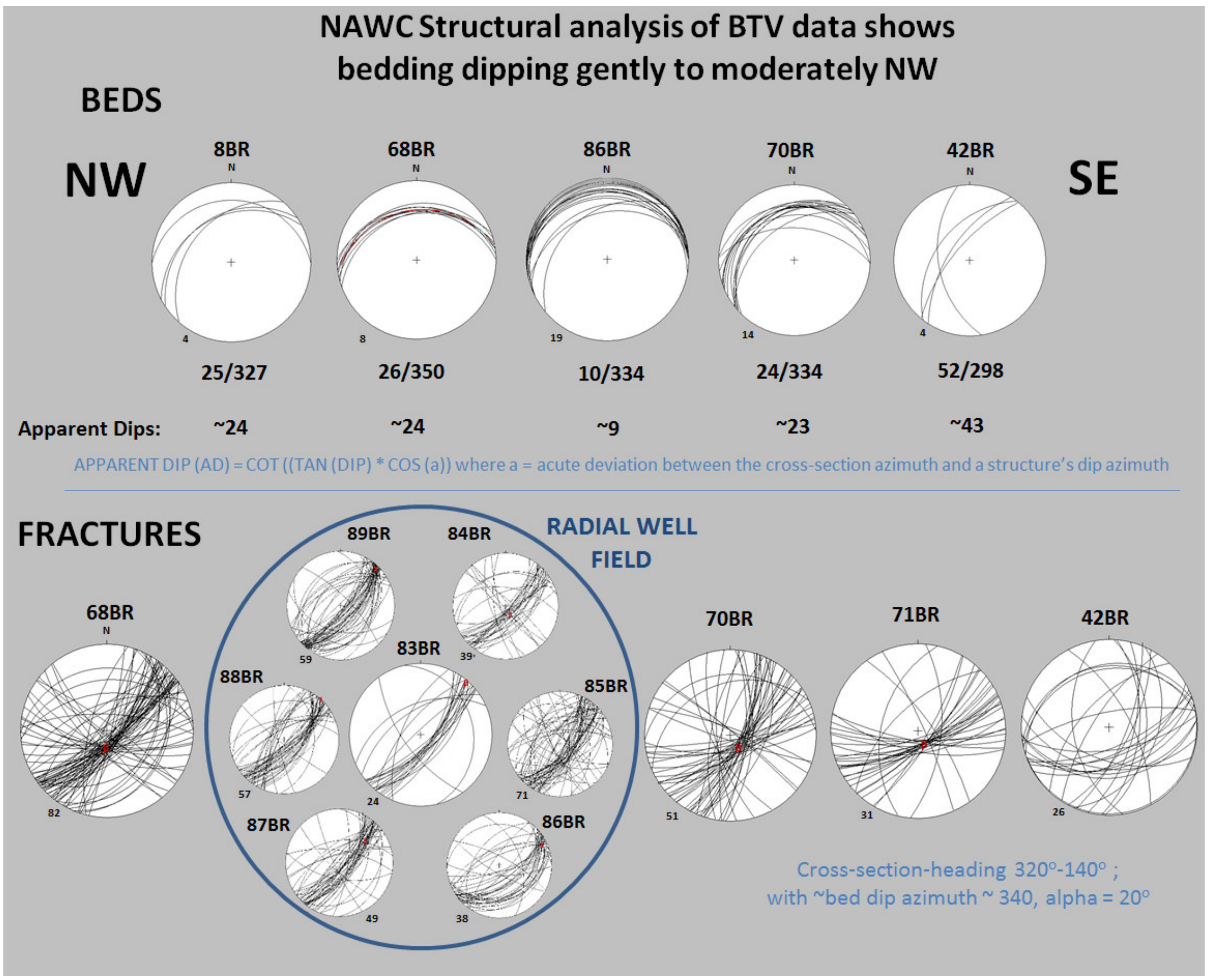

Figure 18: Stereonet structural analyses of BTV data from NAWC. Beds dip gently to moderately NW across the site (top diagrams). Rock fractures are more uniform in orientation (bottom diagram) than for the Stockton Formation at GM-RACER (Figure 17). Note the consistent orientation of rock fractures in the 80BR-series radial wellfield.

-

structural heterogeneity observed for these two sites (Figures 19 and 20) may simply reflect the stratigraphic heterogeneity, with bed and fracture sets in the Stockton Formation displaying much more variability those for those measured in the Lockatong Formation (Figures 15 to 18). Beds and fractures in the Lockatong Formation mostly cluster about the regional strike axis of the basin (S1 of Herman 2007 and Figure 20) and account for almost 1/3 of the total number of fractures measured in this unit. In comparison, S1 fractures in the Stockton Formation are subordinate in abundance to other, more prevalent ones (Figure 19 - S2, S3, SC3 8% trends) that likely reflect later extensional and compressional strains (Herman, 2009)

But these contrasts may simply reflect variable strain responses to the stark sedimentological differences between alluvial beds laid down in the distributary channels of a braided-stream deposit (Stockton) versus those deposited in shallow-to deep lakes and their margins (Lockatong). Consequently, these two sites have very different conceptual hydrogeological frameworks despite being located in such proximity. A

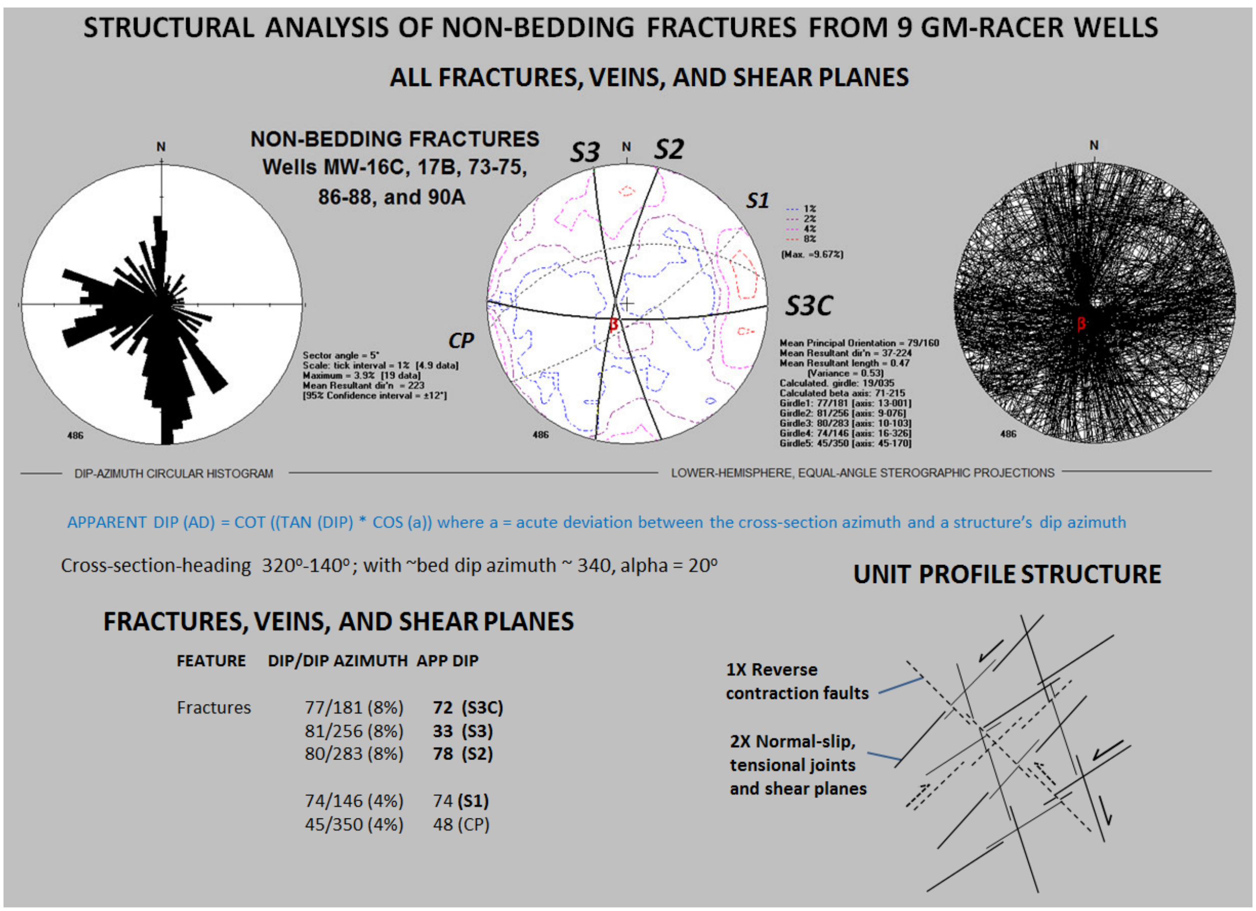

Figure 19: Structural analysis of non-bedding fractures from 9 GM-RACER wells (Table 1). Five principle fracture planes are identified and diagrammed using their apparent dips and relative percentages of the overall fracture population. The three most abundant, representative planes account for only 24% of the fractures measured. These three and two subordinate fracture sets (4%) are represented in profile using their relative abundances to create a unit profile structure (lower right) that is repeated in profile for the cross-section interpretation (Figures 24 and 25).

structural-interpretive process termed 'structural-feature density profiling' was used to illustrate these conceptual differences by developing unit-profile structures for each site that are depicted in Figures 19 and 20. This structural technique was developed over many years while working at the NJGWS and is covered more thoroughly in this year's teacher's workshop (Chapter 1).

Discussion

The reverse faults depicted in map (Figures 3 to 6) and in profile (Figures 24 and 25) are stylized depictions of a penetrative, regional strain field where the Late Triassic section has been contracted and thickened by concealed reverse faults. I initially thought that the autoclastic breccia recovered in the MW-20A core at GM-RACER was an expression of this compressional event and reflected reverse faulting during late-stage basin inversion. The calcite spar from this breccia was sent to Ryan Mathur

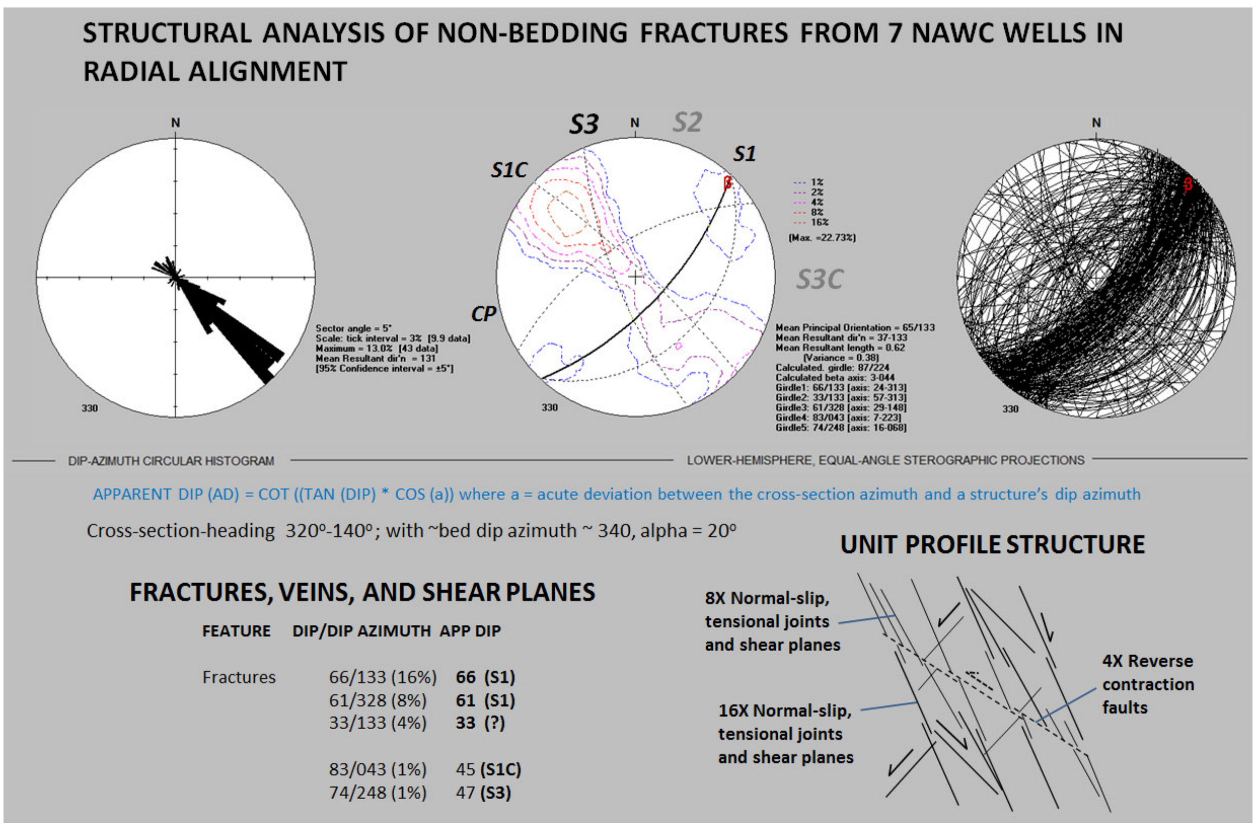

Figure 20: Structural analysis of non-bedding fractures from 7 NAWC wells in radial alignment (Table 1, Figures 6 and 19). Fracture sets measured in this well field were used to construct the representative fracture model for the Lockatong Formation at NAWC. The three most prevalent fractures planes account for 28% of the total number of fractures measured. These three and two subordinate trends (S1C) are combined in relative proportion to create the unit profile structure that is repeated in profile for the cross-section interpretation (Figures 24 and 25)

at Juniata College, Pennsylvania for radiometric dating with the hope that it contained ample uranium and lead isotopes that could define a reliable isochron. But these efforts proved futile as no isotopic traces were found in the submitted samples, and as seen in thin section, this fault breccia was cemented and hardened prior to structural compression. The reverse fault depicted as running southward of the MW-20A core was mapped based on this initial, erroneous assumption, and so revision is already in

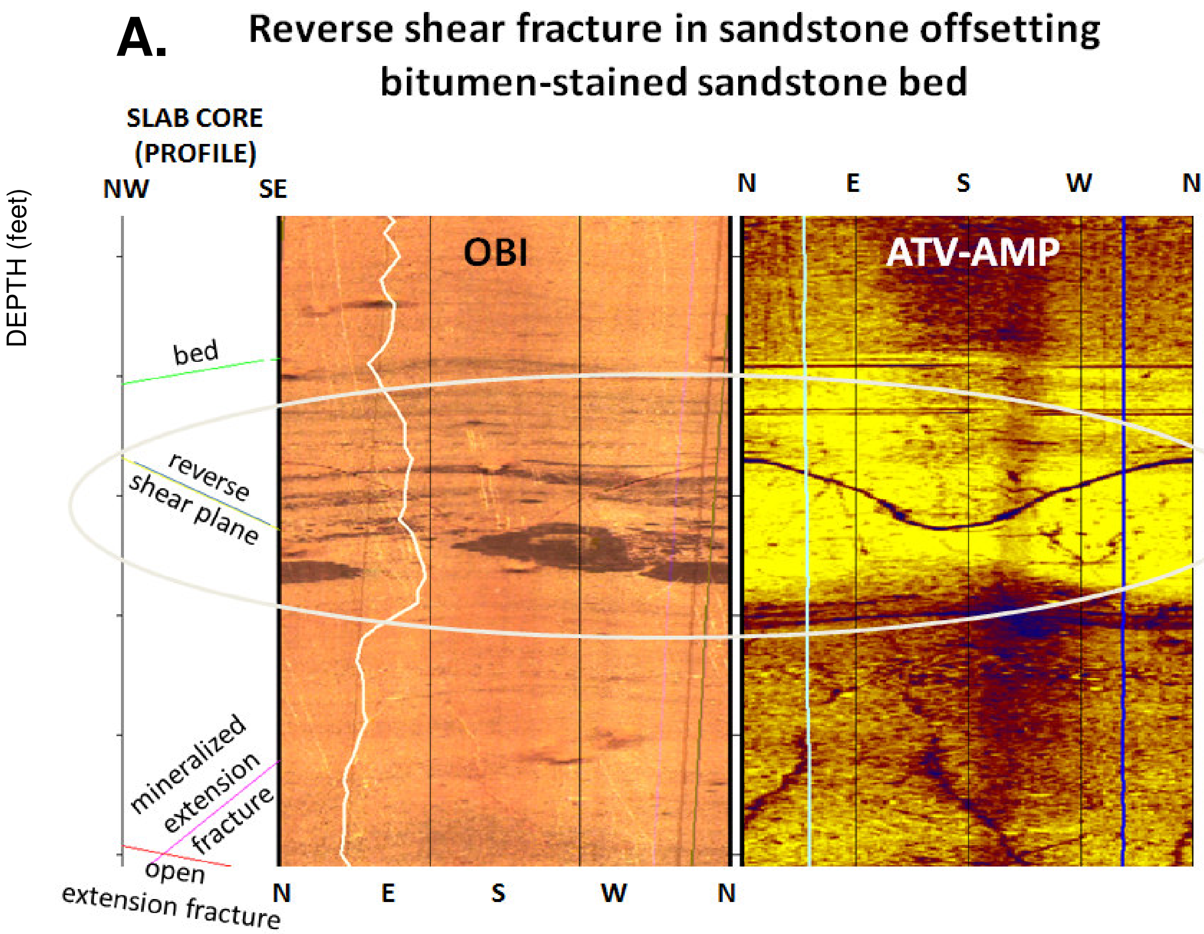

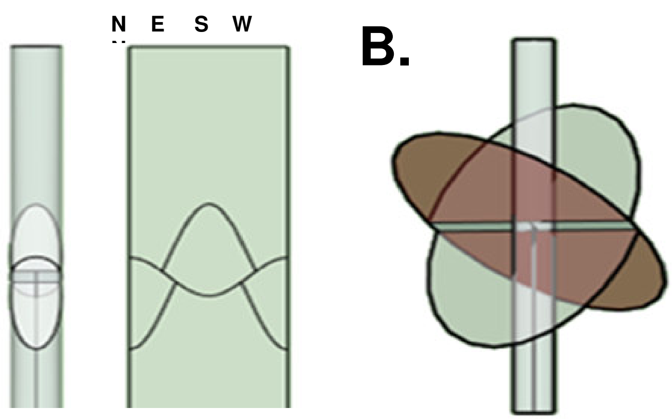

Figure 21: A. Interpreted BTV records for a section of GM-RACER well MW-16C highlighting a late-stage reverse shear plane offsetting bedding and extension fractures. The profile depiction to the left (SLAB CORE) shows the apparent dips of interpreted features. B. A reference diagram showing a reverse-shear plane dipping 45° south offsetting a plane dipping 70° north (see Figure 23).

order. The only well-constrained reverse faults that occur near the surface are those associated with the nearby, overturned beds of Lockatong in Villa Victoria Brook (Field Trip, STOP 3). Representation of the concealed reverse faults for this project therefore relied upon the geometry of local stream corridors where they correspond to abrupt changes in surface-water drainage patterns, for instance where streams take E-W jogs, perhaps coinciding with late-stage fracture swarms or reverse faults of the type that we see glimpses of in excavation and cores but otherwise concealed and therefore inferred on maps owing to the lack of telltale outcrops in the area. The tectonic setting of the Trenton area appears to be unique because I have measured fibrous-quartz-cemented fractures in Lockatong Formations outcrop near Villa Victoria Brook, and have held a hand sample of a quartz-cemented fault breccia, also apparently

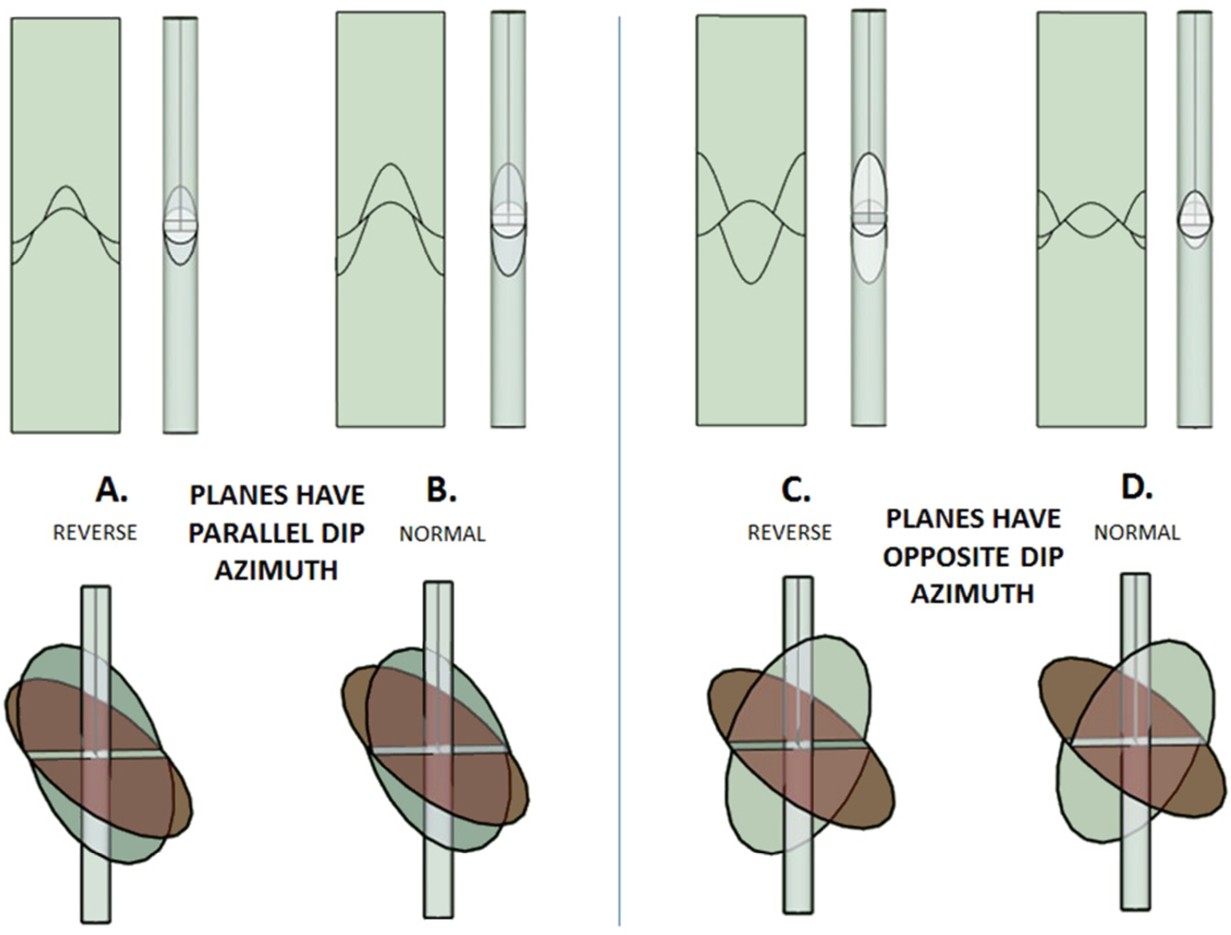

Figure 22: Trimble Navigation, Inc.'s SketchUp 2015 software was used to generate a series of borehole models with shear planes dipping 45o that offset extension fractures dipping 70^{o} and in different directions to serve as a visual aid when interpreting kinematic indicators in BTV records. Each borehole segment was modelled using a 6-inch diameter borehole section that intersects two sorts of cross-cutting planes. The dip separation on each shear plane is 2 inches. After modelling each offset (bottom), the excess area of each plane was trimmed, leaving only the geometric patterns occurring on the borehole walls (top) that were next unrolled and flattened into rectangles using a custom Ruby script by Alexander Schreyer downloaded from the SketchUp Extension Warehouse. The unrolled fracture patterns reveal similar patterns to those seen in BTV records (Figure 21). The four models cover end-member structural scenarios where cross-cutting planes dip in the same (A. and B.) and opposing (C. and D.) directions and have either reverse or normal dip separation.

from the Lockatong Formation that Pierre Lacombe found at land surface near the GM-RACER site. This points to a slightly higher metamorphic grade of Late Triassic rocks in this area with respect to other parts of the basin in New Jersey, but Lucas and others (1988) also report fibrous quartz infilling tectonic veins in the western part of the basin near Jacksonwald, Pennsylvania. It thus seems that the Newark Basin was buried deeply before being 'inverted', or structurally elevated into its current position, with tectonic inversion increasing along the Appalachian grain to the southwest. It's likely that the tectonic episode or

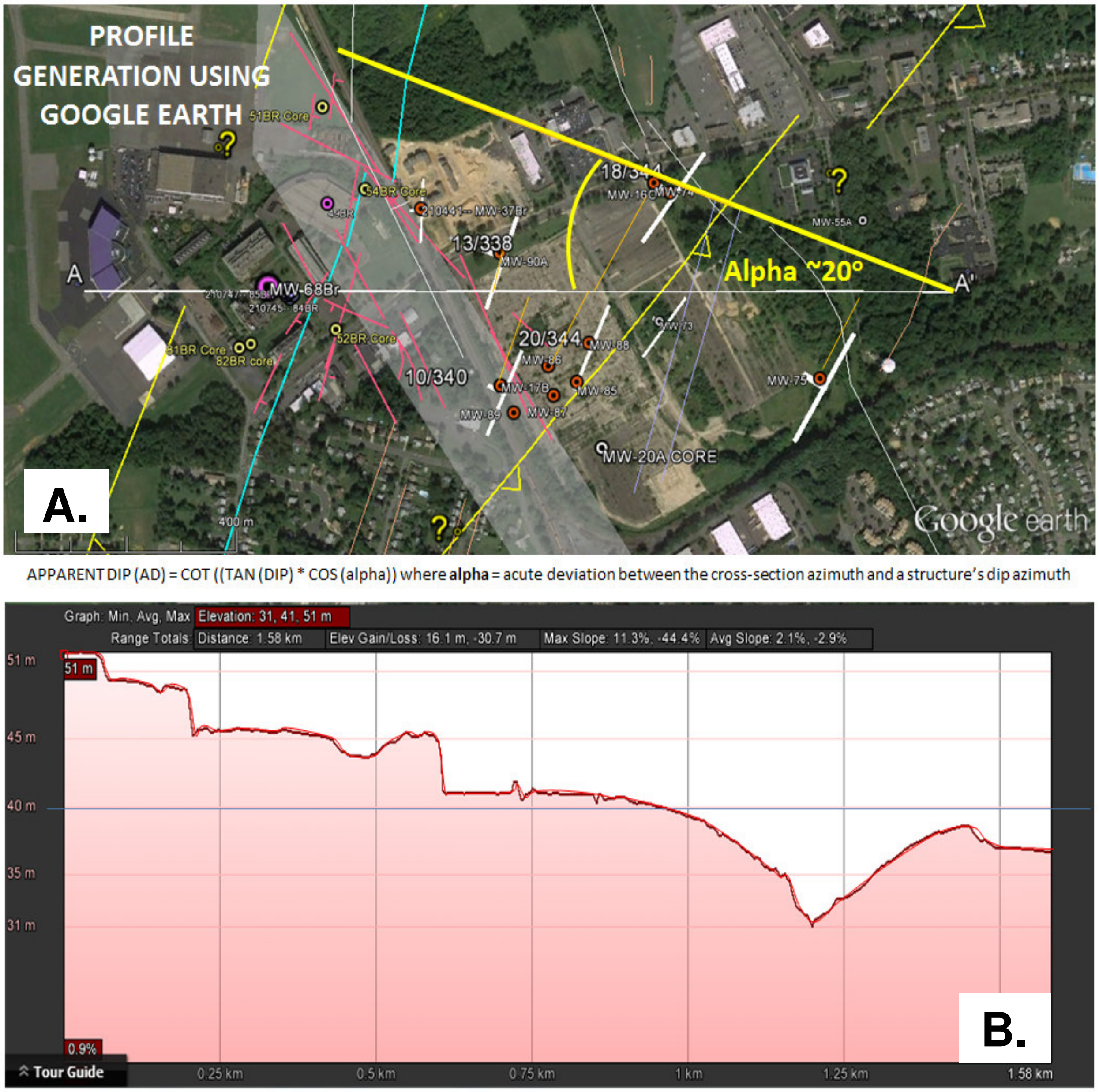

Figure 23: Google Earth (GE) was used to develop cross-section elements including a topographic profile (**B.**) that was auto-generated along the section trace (**A.**). The deviation between dip azimuth and the section trace is also highlighted in **A.** The GE display was captured and placed into MS PowerPoint for tracing with a freeform polyline. The profile topography requires further manipulation to place it into the project with the proper aspect because *it is not captured with equal horizontal and vertical scales* (1:1 scale) and therefore requires manual rescaling. This is further addressed in the Teacher's Workshop (Chapter 1).

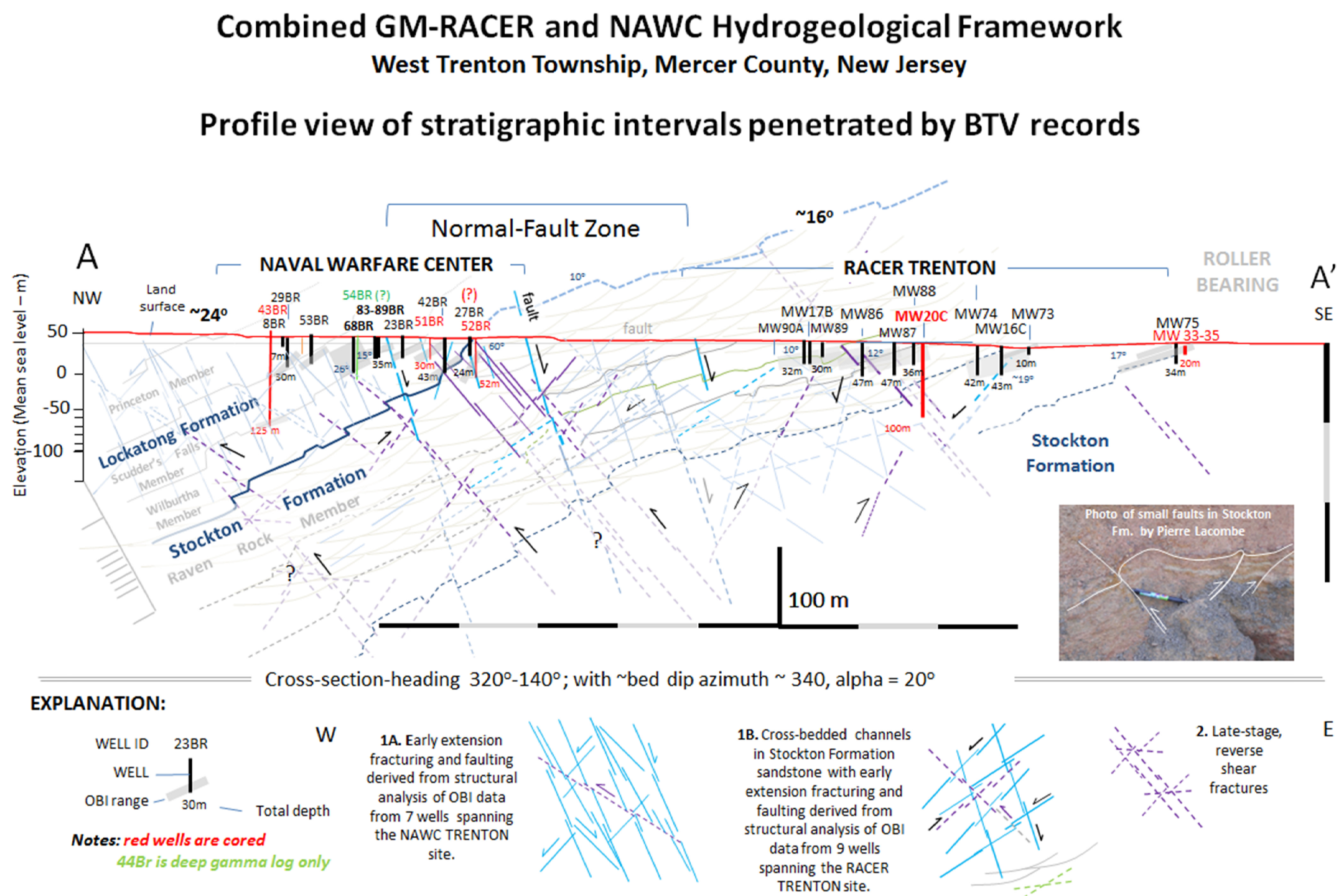

Figure 24: Schematic geological profile detailing the structural style of the area. Please note that not all wells and core are represented owing to graphic cluttering. The 'unit profile structures' (1A. - 1B.) derived in Figures 19 and 20 are repeated as fracture ornamentation in the cross section. Note the similarity between structures seen in the embedded photo (Figure 10B) and the interpreted structural style.

episodes that structurally inverted this section, perhaps by as much as a few kilometers, also overturned the nearby Lockatong beds and imparted mechanical twins to the calcite-spar-cemented autoclastic fault breccia (Figures 9 and 10A) during late-stage tectonic compression after a prolonged, extension-dominated phase of continental rifting (Herman, 2015). The lack of such overturned beds north and east of Trenton and quartz-grade hydrothermal annealing of rock pores lends support to an argument that the compressional strain field increases in intensity southwestward towards Chesapeake Bay (Herman, 2015).

With respect to this conceptual hydrogeological framework, it is important to stress that the contrasting lithologies beneath these two adjacent sites results in very different hydrogeological conditions. The stratigraphic, structural, and hydrogeological contrasts seen between the Stockton and Lockatong Formations has been observed before (Herman, 2010; Herman and Curran, 2010) and result in the former having a much deeper, weathered section than the latter. It is common to see fracture interstices in the Lockatong Formation healed with secondary minerals at depths of only a few meters, whereas fracture interstices and macropores in the Stockton are mostly unhealed or partially open to depths of tens of meters below land surface because any secondary minerals that once filled pores were removed by chemical weathering. This is important to consider when defining the local hydrogeological framework for the conceptual flow model because groundwater flow at significant depths in the Stockton Formation will be less anisotropic than for the Lockatong Formation that behaves as a leaky-multiunit aquifer system like the Passaic Formation (Michalski and Britton, 1997). The difference in primary facture direction

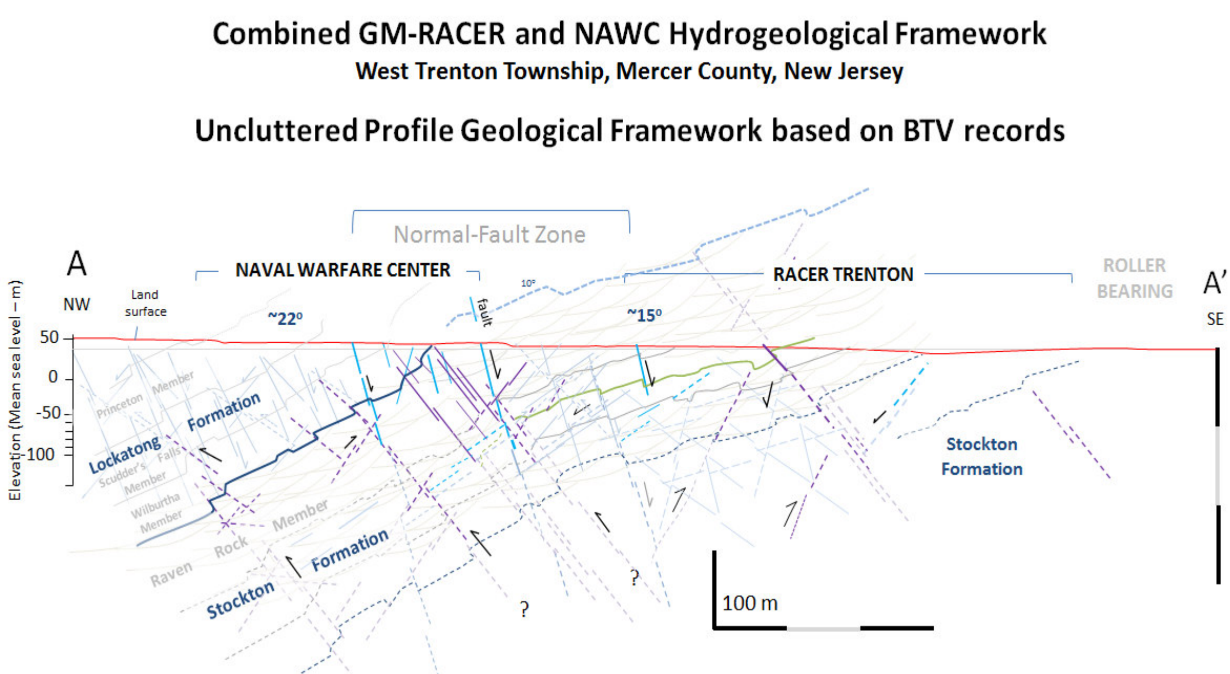

Figure 25: The cross section resulting from this work is clarified by removing all of the well elements and notes thereby emphasizing the conceptual framework for further evaluating the site hydrogeology.

between these two formations is also interesting to note. The Lockatong fractures are predominantly Sub-parallel to the basin-bounding border faults to the northwest (S1 strike group of Herman, 2009). In contrast, the Stockton Formation displays strong N-S and E-W fracture trends, more in line with the strain axes indicted by the regional calcite-strain-gauge data (Herman, 2015). It therefore seems as if the Stockton sandstone behaved rheologically with a relatively higher level of structural competency than the Lockatong Formation, and simply reflects compressional overprinting differently than the argillaceous mudstone and siltstone of the Lockatong.

To conclude, this is the final project that I worked on as a research geoscientist on behalf of the State of New Jersey. There are many remaining geological mysteries to solve in this region, not to mention those that have yet to be unearthed. But the nature of tectonics in the Trenton area has been variously interpreted and depicted in modern times, and it is important to pay attention to new excavations and opportunities like this to acquire the kind of shallow subsurface information that can advance our understanding of complex geological systems in a realistic manner. After decades of mapping geology in New Jersey I have come to greatly admire the ancient practitioners that reported only what they saw and inferred little. But science is speculative by nature and as we continue to push boundaries, a cautious approach is warranted that employs established scientific methods because of the complex, deeply weathered and concealed nature of the bedrock in this region. The system of normal faults cutting through this region as depicted by Owens and others (1998) is stylistic and flawed, and in need of more 1:24,000-scale refinement. Surface-water drainages follow inherent weaknesses in bedrock corresponding to intervals, or zones of relatively dense fracturing and faulting (Ackerman and others, 1997). The steeply dipping rock joints that we see at the surface impart bulk shear in competent rock during extension and collapse of this thick pile of rift-basin fill (Herman, 2009), and so it becomes a matter of degree to where fault zones versus dense fracture zones are mapped. But this work has laid the groundwork for further investigations that should examine the depth of fracture healing in more detail with respect to observed groundwater flow at each site. The geological nature and extent of this area has historically been elusive, but it is further elucidated here using BTV and core records in an integrated, synoptic approach. Many such complex groundwater-pollution cases occur in this region, and as we deploy better tools in an effort gain a firmer foothold on the hydraulic nature of complex aquifers, this type of approach may prove valuable elsewhere in deciphering just how fractured-bedrock holds and transports groundwater and its contaminants.

References

Ackermann, R. V., Seidl, M. A., Schlische, R. W., 1997, First-order structural controls on modern drainage networks within the Newark rift basin, New Jersey: Geological Society of America Abstracts with Programs, v. 29, n. 1, p. 25

Berg, T. M., Edmunds, W. E., Geyer, A. R., and others, compilers, 1980, Geologic map of Pennsylvania: Pennsylvania Geological Survey, 4th ser., Map 1, 2nd ed., 3 sheets, scale 1:250,000.

Coffin M. F., and Eldholm, O., 1994. Large igneous provinces: crustal structure, dimensions, and external consequences: Reviews of Geophysics, vol. 32, p. 1-36.

Engelder, T., 1979, The nature of deformation within the outer limits of the central Appalachian foreland fold and thrust belt in New York State, Tectonophysics, 55, 289-310.

Goode, D. J., Imbrigiotta, T. E., and Lacombe, P. J., 2014, High-resolution delineation of chlorinated volatile organic compounds in a dipping, fractured mudstone: Depth- and strata-dependent spatial variability from rock-core sampling: Journal of Contaminant Hydrology, v. 171, p. 1-11.

Herman, G. C., 2015, Neotectonics of the New York Recess, *in* Herman, G. C., and Macaoay Ferguson, S., eds., Neotectonics of the New York Recess: 32nd Annual proceedings and field guide of the Geological Association of New Jersey, Lafayette College, Easton, Pa., p. 80-151 (16.0 MB)

Herman, G. C., 2010, Hydrogeology and borehole geophysics of fractured-bedrock aquifers (5 MB PDF), *in* Herman, G. C., and Serfes, M. E., eds., Contributions to the geology and hydrogeology of the Newark basin: N.J. Geological Survey Bulletin 77, Chapter F., p. F1-F45.

Herman, G. C. and Curran, J. F., 2010, Borehole geophysics and hydrogeology studies in the Newark basin, New Jersey (38 MB PDF), *in* Herman, G. C., and Serfes, M. E., eds., Contributions to the geology and hydrogeology of the Newark basin: N.J. Geological Survey Bulletin 77, Appendixes 1-4, 245 p.

Herman, G. C., 2009, Steeply-dipping extension fractures in the Newark basin (5 MB PDF), Journal of Structural Geology, V. 31, p. 996-1011.

Herman, G. C., 1997, Digital mapping of fractures in the Mesozoic Newark basin, New Jersey: Developing a geological framework for interpreting movement of groundwater contaminants: Environmental Geosciences, v. 4, no. 2, p. 68-84.

Herman, G.C., Dooley, J.H., and Mueller, L.F., 2010, Geology of the Pennington Trap Rock (Diabase) Quarry, Mercer County (6 MB PDF), *in* Lacombe, Pierre, ed., Geology of Trenton and its impact on the Capitol City: 27th Annual Meeting of the Geological Association of New Jersey, Trenton, NJ, p. 92-119.

Lewis-Brown J. C., and Rice, D. E., 2002, Simulated ground-water flow, Naval Air Warfare Center, West Trenton, New Jersey: U.S. Geological Survey Water-Resources Investigations Report 02-4019, 44 p.

Lacombe, P.J., 2000, Hydrogeologic framework, water levels, and trichloroethylene contamination, Naval Air Warfare Center, West Trenton, New Jersey, 1993-97: U.S. Geological Survey Water-Resources Investigations Report 98-4167, 139 p.

Lacombe, P.J., 2001, Water levels and potentiometric surfaces, Naval Air Warfare Center, Trenton, New Jersey, 2000: U.S. Geological Survey Water-Resources Investigations Report 01-4197,46 p.

Lacombe, P.J., and Burton. W., 2010. Hydrogeologic framework of fractured sedimentary rock, Newark Basin, New Jersey. Groundwater Monitoring & Remediation V. 30, no. 2, p. 35–45.

Lomando, A. J. and Engelder, Terry, 1984, Strain indicated by calcite twinning: Implications for deformation of the Early Mesozoic Northern Newark Basin, New York: Northeastern Geology, vol. 6, no. 4, p. 192-195.

Marzoli, A., Renne, P., Piccirillo, E., Ernesto, M., Bellieni, G., and De Min, A, 1999. Extensive 200-million-yearold continental flood basalts of the Central Atlantic Magmatic Province: Science v. 284, p. 616–618.

Michalski, Andrew, and Britton, Richard, 1997, The role of sedimentary bedding in the hydrogeology of sedimentary bedrock - Evidence from the Newark Basin, New Jersey: Ground Water, Vol. 35, No. 2, p. 318-327.

Robinson, J., Slater, L., Johnson, T., Shapiro, A., Tiedeman, C., Ntarlagiannis, D., Johnson, C., Day-Lewis, F., Lacombe, P., Imbrigiotta, T., and Lane, J., 2015, Imaging pathways in fractured rock using three-dimensional electrical resistivity tomography: Groundwater, v. 54, Issue 2, p. 186–20.

Owens, J. P., Sugarman, P. J., Sohl, N. F., Parker, R. A., Houghton, H. F., Volkert, R. A., Drake, A. A., Jr., and Orndorff, R.C., 1998, Bedrock Geologic Map of Central and Southern New Jersey, U. S. Geological Survey Miscellaneous Investigation Series Map I-2540-B, scale 1:100,000, 4 sheets.

Acknowledgements

This study was facilitated by the cooperative efforts of the USGS Water Science Center in Trenton, NJ, by Haley-Aldrich, Inc. from their Cleveland, OH and Parsippany, NJ offices, and by Hager-Richter, Inc. out of their Fords, NJ office. Accordingly, I am sincerely grateful to Pierre Lacombe, Emmanuel Charles, and Alex Fiore of the US Geological Survey, to Dimitri Quafsi of Haley-Aldrich and Rob Garfield of Hager-Richter for providing the BTV data records, reports, maps, photographs, and core samples for inspection and interpretation. This project could not have happened without their contributions.